Monitoring and Analysis of Trace Metals in Coastal and Transitional Waterways

Martin Nolan, BSc

Submitted for the award of MSc by Research

Dublin City University

Supervised by Dr. Blánaid White & Prof. Fiona Regan

School of Chemical Sciences

July 2020

Declaration of Academic Integrity

I hereby certify that this material, which I now submit for assessment on the program of study leading to the award of MSc by Research is entirely my own work, and that I have exercised reasonable care to ensure that the work is original, and does not to the best of my knowledge breach any law of copyright, and has not been taken from the work of others save and to the extent that such work has been cited and acknowledged within the text of my work.

Signed: _____

ID Number: 13509017

Date: _____

Table of Contents

Abbreviations

AA-EQS	Annual Average Environmental Quality Standards
AAS	Atomic Absorption Spectroscopy
AdSV	Adsorptive Stripping Voltammetry
APA	Agarose Crosslinked Polyacrylamide
ASV	Anodic Stripping Voltammetry
BFE	Bismuth Film Electrode
BLM	Biotic Ligand Model
CCE	Carbon Counter Electrode
CNT	Carbon Nanotubes
CRM	Certified Reference Material
CSV	Cathodic Stripping Voltammetry
CV	Cyclic Voltammetry
DBL	Diffusive Boundary Layer
DGT	Diffusive Gradients in Thin Films
DIFS	DGT Induced Fluxes in Sediment
DO	Dissolved Oxygen
DOC	Dissolved Organic Carbon
DOM	Dissolved Organic Matter
DMG	Dimethylglyoxime
DPV	Differential Pulse Voltammetry
EPS	Extracellular Polymeric Substances
EQS	Environmental Quality Standards
FIAM	Free Ion Activity Model
GCE	Glassy Carbon Electrode
GEP	Good Ecological Potential

GES	Good Ecological Status
GPES	General Purpose Electrochemical System
HDPE	High Density Polyethylene
HMDE	Hanging Mercury Drop Electrode
ICP	Inductively Coupled Plasma
ICP-MS	ICP-Mass Spectrometry
ICP-OES	ICP-Optical Emission Spectrometry
LOD	Limit of Detection
LOQ	Limit of Quantitation
LDPE	Low Density Polyethylene
MFE	Mercury Film Electrode
PC	Polycarbonate
PES	Polyethersulphone
PET	Polyethylene Terephthalate
PMMA	Polymethyl Methacrylate
PSD	Passive Sampling Device
ROS	Reactive Oxygen Species
SD	Standard Deviation
SEM	Scanning Electron Microscopy
SWI	Sediment-Water Interface
SWV	Square Wave Voltammetry
TBT	Tributyltin
TEL	Tetra-Ethyl Lead
UV	Ultraviolet
WFD	Water Framework Directive

List of Figures

List of Tables

Acknowledgements

Abstract

Monitoring and Analysis of Trace Metals in Coastal and Transitional Waterways

Martin Nolan

Heavy metals are of particular concern as environmental contaminants due to their toxic effects when accumulated within organisms. Under the European Union Water Framework Directive (WFD) 2013/39/EU, cadmium (Cd), nickel (Ni) and lead (Pb) were identified as priority metals of ecological concern which must be mediated to achieve a good environmental status. Widespread implementation of these regulatory policies requires the use of accurate monitoring and analytical techniques, which are often costly, and are a barrier to compliance in some cases. As such, there is a need to further develop and validate low-cost and easy-to-use monitoring and analytical protocols.

Passive sampling devices (PSDs) allow for the accumulation of an analyte over time, providing a time weighted average of analyte concentrations in a water body. For heavy metals in solution, the most prominent PSD is the Diffusive Gradients in Thin Films (DGT) device. DGTs measure a fraction of labile metals, often considered to be equivalent to the bioavailable fraction. Such PSDs require definition of appropriate Environmental Quality Standards (EQS) prior to their wider use in a regulatory context. Electrochemical analysis techniques such as stripping voltammetry may be used to analyse trace metals and are cheaper to use and run than traditional metal analysis instrumentation, and can be easily modified to optimise for certain analytes.

In this thesis, the potential for the application of PSDs and stripping voltammetry in monitoring programs was advanced. A review of current trace metal monitoring techniques and comparative studies using DGT were presented. Stripping voltammetry was examined as a method of analysis of coastal and estuarine water samples. The impact of biofouling on DGTs was also examined in marine and transitional waters across the Atlantic coast, evaluating speciation and extent of fouling. Taken together, these findings help inform future trace metal monitoring and remediation programs.

Chapter 1

Monitoring Trace Metals as Contaminants of Emerging Concern:
Towards the Use of Passive Sampling Devices

1.1 Introduction

Trace metals are ubiquitous in the environment, and some metals are essential for optimal growth and development of organisms. Essential metals such as copper (Cu), iron (Fe), manganese (Mn) and zinc (Zn) are often described as micronutrients and are critical in normal biological function for many organisms.[1] However, high concentrations of these micronutrients can negatively impact the health of biota, and other non-essential metals such as arsenic (As), lead (Pb), cadmium (Cd) and mercury (Hg) serve no ecological benefit and can directly cause toxicity.[2]

Many organisms exposed to waters or sediment enriched with trace metals can accumulate these contaminants in their tissues, in a process known as bioaccumulation. Aquatic plants and algae, invertebrates such as mussels and oysters, and fish may all accumulate trace metals following exposure.[3–5] These organisms accumulate metals via different pathways, which will be discussed in more detail in Section 1.3. While acute toxicity may occur following rapid and severe contamination events, leading to death of organisms and changes in overall biodiversity, chronic toxicity may occur as a result of low levels of exposure to trace metals over extended periods. Non-essential metals such as Cd, Pb, and Hg may persist in tissue and bone for years and pose a continuing risk of chronic toxicity.[6] Terrestrial organisms such as livestock which drink from contaminated waters may similarly accumulate trace metals.[7]

In a comprehensive review of the biological effects of common-non essential metals by Tchounwou *et al.*, the impact of metal cations substituting elements in biological processes was detailed.[1] For example, Pb may be deposited in bone in place of calcium (Ca) and competes with other essential metal cations.[1] Metals such as As cause toxicity in plants by replacing phosphate in biochemical reactions, but some plants express genes for As resistance, such as the ACR3 gene.[3] Many of the toxic and carcinogenic effects of trace metals occur due to the induction of stress pathways and the formation of reactive oxygen species (ROS), and can even be caused by high concentrations of essential metals such as Cu and Fe.[1,8,9] A review by Egorova & Ananikov summarised the toxicity of some metal species in relation to other metal compounds.[8]

To safeguard the health and biodiversity of waterways, it is essential that environmental contaminants such as heavy metals are monitored, and the impact of further contamination events reduced. Increasing concern regarding the ecological status of European water bodies led to the development of the EU Water Framework Directive (2000/60/EC), or WFD.[10] The WFD initially aimed for all rivers, lakes, transitional and coastal waters of EU member states to achieve a Good Ecological Status (GES) by 2015, through monitoring and management of highlighted priority contaminants. In the 2013 amendment (2013/39/EU), this goal was revised, with the Environmental Quality Standards (EQS) for original priority substances to be met by 2021, and EQS for newly introduced priority substances by 2027.[11] Four metals and their associated compounds are included on the original priority substances watchlist: Cd, Hg, Pb, and nickel (Ni).[10]

The GES metric is assessed by evaluating many factors of the water body, including the concentrations of priority substances, biodiversity, physico-chemical parameters, and hydrodynamics due to morphological elements. Ecological quality assessment alongside trace metal analysis can provide some insight into how these contaminants may affect the overall environmental status. In a study by Simboura *et al.*, strong correlations between Cd contamination and poor ecological status were noted, and in general there were lower metal concentrations at sites achieving GES.[12] Assessment of the environmental status of a waterway also involves the consideration of the site's natural and man-made morphological features. Semi-enclosed bays and lagoons and constructed harbours may cause trace metals and other contaminants to persist locally for longer periods than open sites due to their atypical hydrodynamics.[13,14] Heavily modified or artificial water bodies are assessed differently under the WFD, using a Good Ecological Potential (GEP) metric in place of GES.[10] Full implementation of the WFD requires mediation of environmental impact of priority contaminants, and therefore the understanding of their input processes and their fate in the ecosystem is essential.

1.1.1 Processes of Trace Metal Contamination

Trace metal contamination can arise in waterways as a result of a wide range of natural and anthropogenically-driven processes. While high concentrations of a given metal may be indicative of a contamination event, other factors such as the natural background concentrations at a given site must also be considered. Due to localised

geological compositions, every site has a background metal concentration and hence no environmental water body can be classified as entirely pristine. When a water body is near to metal-enriched features such as ore deposits, the concentrations of trace metals in the water can be hundreds or thousands of times greater than similar water bodies without enrichment.[15] Runnells *et al.* reviewed data from various surface and shallow groundwater studies and highlighted variations in pH and metal concentration due to local geology.[15] Other studies suggest that volcanic regions exhibit heightened background concentrations of chromium (Cr), and the weathering of igneous rocks such as alkaline basalt can result in Fe enrichment.[16] It may be challenging to evaluate the geological influence on trace metal concentrations of larger water bodies, however, due to anthropogenic inputs and natural redistribution events.

Weather conditions can lead to enrichment or dilution of trace metals in waterways. Heavy storms can increase trace metal concentrations by resuspending sediment, potentially releasing particle-bound trace metal species in the process.[14] Heavy rainfall can result in run-off of anthropogenic contaminants from terrestrial sites, and acidic rains can result in weathering of rocks, leading to metal enrichment in the runoff.[16] As weather conditions vary depending upon the season of sampling, there can be seasonal variations in trace metal concentrations and the tissues of biota in the water body. The impact of seasonality on metal concentrations is debated; some researchers, such as Li *et al.* and Papafilippaki *et al.*, suggest that higher trace metal concentrations in water occur in summer, potentially as a result of increased agricultural input and higher temperatures increasing degradation of organic matter.[17,18] Other research by Prange & Dennison found higher concentrations of trace metals in sampled seagrass during winter months, correlating with higher rainfall.[19] The uncertainty introduced by weather conditions highlights the necessity of longer-term monitoring programs for accurate interpretation, as sampling performed after a severe weather event (such as heavy rains inducing surface runoff of contaminants) may not reflect the true ecological status of a water body.

Large-scale redistribution events, such as ocean currents and atmospheric cycling, further complicate interpretation of the sources of contamination, as the effects of these events may be present hundreds of kilometres from the source. Degassing volcanoes can result in substantial releases of aerosol and particulate forms of Hg and

Cd into the atmosphere.[20,21] Saharan dust storms, caused by sand particles carried by strong winds, can lead to the enrichment of Fe and Mn in water bodies such as the Mediterranean Sea and the North Atlantic Ocean. Metals from such events, as well as from anthropogenic sources, may be dispersed in the atmosphere as highly soluble aerosols and can result in heavy metal enrichment a great distance from the initial contamination event.[22] When metals are dissolved in ocean waters, they can be transported extended distances by ocean currents. For example, Illuminati *et al.* suggest that high metal concentrations in the tissues of Antarctic sponges may be in part due to the movement of trace metals by the Antarctic Circumpolar current.[23]

Anthropogenic sources of contamination are most traditionally considered to result in decline in environmental status. Rapid advances in industrialisation globally in the past century has led to increased anthropogenic pressures on the surrounding environment. Mining, agriculture, and other industries have caused widespread dispersal of trace metals in the environment, with notable increases in these pollutants in waterways since the start of the 20th century.[2] Sediment core analysis performed in multiple regions indicates heightened trace metal concentrations in the 1960s and 1970s, in line with increasing global industrial pressures.[24] High population density and development along waterfronts results in contamination due to pollutants such as waste effluent from industry and water treatment, and combustion of fuel. Redevelopment of coastlines may also affect the hydrodynamics of the coast, affecting the biodiversity at the site. Studies such as the meta-analysis by Sánchez-Quiles *et al.* highlight the impact of urbanisation of coastlines on biota in regions such as the Mediterranean coast.[3]

During the 20th century, several innovations incorporating metals led to global metal pollution. In the 1920s, tetra-ethyl lead (TEL) was first added to petrol to improve fuel efficiency and performance of engines. Use of leaded fuel spread globally, and between 1925 and 1990, 90% of atmospheric Pb originated from leaded fuel combustion.[25] Due to the significant negative impact of leaded fuel on both human and environmental health, it was formally banned in the EU by Directive 98/70/EC,[26] and as of 2019 the only country that maintains widespread leaded fuel use is Algeria. Isotopic forms of Pb can be used to identify legacy contamination issues related to leaded fuels, as much of the TEL used in these fuels was produced using ore originating from a small number of mines.[27] Similarly, tributyltin (TBT) was used as

an additive to biocidal paints to prevent biofouling on ships. If left untreated, biofouling would lead to reduced fuel efficiency due to increased weight, increasing cost of haulage. However, TBT readily leached from the biocidal paints and was toxic to many non-target marine organisms,[28] leading to its ban under an International Maritime Organization treaty in 2001.

While few metal contaminants have as pronounced an impact on environmental status as TBT and TEL, the use of metals in many everyday products and applications has caused widespread anthropogenic contamination.[1] Cd is released during the combustion of fuels such as coal and oil,[24] is a by-product of the production of steel, and can be present in some phosphorite-based fertilizers.[12] Following the ban of TBT, Cu and Zn biocidal paints saw widespread use on ship hulls. While these paints are a more environmentally friendly option, leaching of these trace metals can lead to localised concentration in harbours and marinas.[29,30] Cu-based fungicides are also used to protect crops from infection and damage.[31] Ni and vanadium (V) are present in crude oil and often uses as markers when assessing the ecological impact of oil spills. For example, the large-scale Deepwater Ocean spill in 2010 resulted in heightened concentrations of sediment-bound Ni at the southern Florida coast.[32] Aluminium sulphate (alum) is commonly used in wastewater treatment to aid removal of particles, and is released among the effluent.[33] The widespread and diverse use of metals leads to contamination of waterways, soils, and air, and European atmospheric trace metal pollution primarily consists of Cd, Cu, Ni and Zn that can be resuspended in the water column.[34] Given the extensive used and varied applications of metals, and the redistribution events that can occur as described previously, anthropogenic pollution is of major concern to the health of waterways and the impact of single factors can be challenging to estimate without rigorous sampling campaigns.

1.2 Direct Sampling Methods

1.2.1 Water Sampling

A basic method of water quality assessment at a given time and location is to perform direct grab sampling of the water. Grab sampling can be performed with relative ease and provides the localised concentration of contaminants in the water at a given instant. Frequent sampling at different points in a water body can be used to identify abrupt changes in water status, helping to identify and determine the impact of an

acute contamination event when it occurs. Using samplers such as Niskin bottles, water samples can be taken at various depths to obtain a depth profile of contaminant distribution.

When assessing the ecological risk of trace metals in solution, the speciation of the metal is a critical factor. Trace metals in solutions may be adsorbed to particles or colloids, may form complexes with organic and inorganic ligands, or may be present as free ions.[35,36] While samples are stored, the speciation of metals may change, and metals may adsorb to organic matter, colloids and particles present in the sample. If the storage vessel is made of certain plastics, trace metals may also adsorb to the walls.[37] By filtering water following sampling, information regarding speciation can be determined. Under the WFD, passing water through a filter of pore size 0.45 µm is representative of the dissolved fraction, removing particulate matter and larger colloidal forms.[10] If unfiltered fractions are retained and analysed alongside filtered samples, grab sampling can be used to provide dissolved, particulate, and total trace metal concentrations at a given instant.[35,38]

Environmental waters are often enriched with dissolved organic matter (DOM) and particulate organic matter, which act as organic ligands with which trace metals can readily form complexes.[39] In a study of humic acid (a major constituent of DOM in environmental waters) complex formation with trace metals at a range of salinities, 65% of Pb and 99% of Hg free ions formed complexes across the studied salinity range.[40] Cu and Ni form strong bonds with organic ligands and these complexes are more inert than most bioavailable metal complexes.[35,41,42] Speciation in solution is complex and varied; a schematic of the transformation free ions may undergo is displayed in Figure 1.1.
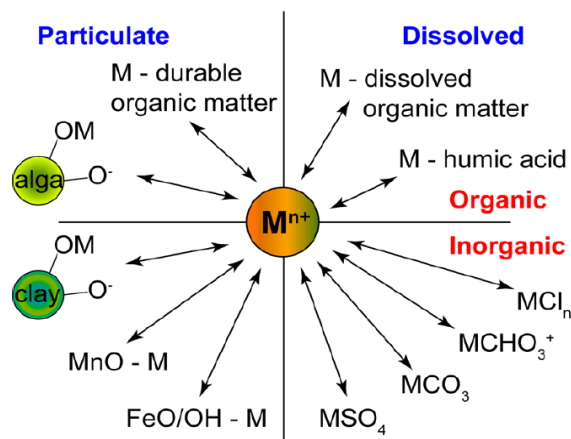
Figure 1.1: Potential transformation pathways of free metal ions (M) in solution and complexes they may associate with. Reproduced from Egorova and Ananikov.[8]

Physico-chemical parameters of a water body such as pH and redox potential can affect the speciation of metals in solution and alter subsequent biological uptake.[39,43] The pH of bulk solution can affect solubility of many metals, such as aluminium (Al), which forms insoluble hydroxide complexes in neutral waters.[8,44] Cr is available to biota as the Cr^{3+} free ion, but in highly oxygenated waters above pH 7, the Cr^{6+} form is dominant as part of the CrO_4^{2-} anion.[35] Lipophilic complexes, which generally can readily diffuse into cells, may have reduced uptake into cells at low pH due to reduced electrostatic force between phospholipids. Dissolved oxygen (DO) content of water also affects speciation, oxidising soluble metals such as Fe^{2+} and Mn^{2+} into colloidal forms.[45] These colloidal metal oxides may then result in antagonistic interactions with other metals, binding other species.[46] The impacts of physico-chemical parameters, metal interactions with ligands and other metals, and varying pathways of metal internalisation result in difficulty in determining overall biological risk of trace metals in solution.

Trace metal analysis of some water samples may be challenging due to matrix effects of the sample, which will negatively affect the detection limits of common metal analysis instrumentation. The sensitivity of Inductively Coupled Plasma (ICP) and Atomic Absorption Spectroscopy (AAS) systems are reduced when analysing high-salinity waters coastal or oceanic waters, or water from sites with high organic matter content (such as marshes). Interferents including sodium (Na), potassium (K), calcium (Ca) and chlorine (Cl) are often present in high concentrations in seawater,

greatly exceeding concentrations of trace metals of interest. Pre-concentration steps are often necessary when analysing such samples, methods have been developed for seawater analysis using Chelex 100 chelating resin to isolate analytes of interest from the matrix.[47] This pre-concentration method can be performed with direct feeds into systems such as ICP, removing a potential contamination step due to manual handling.[48] Other metal analysis methods such as stripping voltammetry may be used to determine free ionic or weakly complexed metals, but can similarly be affected by certain sample types. Organic matter from water samples may adsorb to the electrode during stripping voltammetry and may form complexes with metal of interest, leading to underreported concentrations and potential misidentification of metals due to peak shifts.[49] As such, in the case of organic-rich water samples, UV irradiation is performed to destroy organic matter prior to analysis.

A major disadvantage of direct grab sampling is the resolution of the sampling, as the sampling provides data regarding the concentration of contaminants at the very instant sampling is performed. Often, water bodies are highly dynamic, and subject to significant variations in concentration over short periods of time.[41,50] At estuarine sites, for example, tidal activity leads to fluctuations in suspended metal concentrations.[51] Long-term and frequent monitoring of water bodies would be required to achieve truly representative results using this method, accounting for variable factors such as the impact of weather events on concentrations. In many cases, the concentrations of trace metals may be too low in bulk water samples for accurate quantitation using analytical instrumentation, and pre-concentration steps may be required as above in order for the limits of quantitation to be reached. The method is also prone to contamination during processing due to the many steps required to obtain representative results. Nevertheless, the simplicity of sampling method makes this method a useful option, particularly when validated with a secondary sampling method.

1.2.2 Sediment Sampling

Metals suspended in the water column may eventually become incorporated in the bottom sediment of a water body. Sediment acts as an effective sink for both toxic and essential trace metals,[9,52] and enriched sediment is a pathway of trace metal uptake by many aquatic organisms including deposit and filter feeding invertebrates and rooted macrophytes.[45,53] Due to the accumulation of trace metals over time, sediment

samples typically exhibit higher trace metal concentrations than the water column, and may be more representative of a time-integrated environmental status of the waterway.[13] As discussed previously, sediment core analysis can allow for estimation of trace metal contamination decades prior to sampling.[24]

The trace metal accumulation potential of a sediment bed, and the availability of contaminants within to biota, is dependent upon many factors. Physical parameters such as particle size and type (silt, sand, etc.), and the organic matter content influence the accumulation potential of the sediment bed.[54] The sediment can be perturbed by factors such site hydrodynamics, weather events, burrowing organisms, and boating activity, resuspending particles and releasing reactive particle-bound metals which organisms in the water column may subsequently be exposed to.[55,56] Physico-chemical parameters such as pH and dissolved oxygen (DO) in the sediment can influence the speciation and the availability to biota of metals in the sediment and its porewaters. Microbial activity and other biochemical processes can lead to localised fluctuations of these parameters, causing localised speciation changes. In regions of high DO, free ion metal species such as Fe^{2+} and Mn^{2+} may be oxidised to insoluble oxyhydroxide forms, and be reduced back to free ions in suboxic or anoxic regions of the sediment.[45] Processes such as the degradation of the organic matter in the sediment can also lead to the release of reactive metal species. The processes that continuously occur in the bottom sediment lead to constant changes in metal speciation, and hence it is not possible to accurately determine the speciation of the metals within the sediment.

Extraction of trace metals can be performed by microwave acid digestion to quantify acid-extractable metals, or by the addition of chelating agents such as EDTA. Subsequently, standard methods such as ICP and AAS can be used to analyse the eluate.[57] The time-integrated concentration of trace metals and extraction processes make sediment sampling a useful alternative to water sampling when working with less sensitive instrumentation with higher limits of detection. For example, cheaper optical emission spectrometry ICP (ICP-OES) systems can be used in place of mass spectrometry ICP (ICP-MS) due to the higher concentrations in the sediment eluate. However, it is difficult to determine availability to biota, resuspension potential, speciation, or toxicity from this process, providing only total metal concentrations.[57] Nonetheless, sediment trace metal concentrations may provide insight into the

environmental status of the site, and the simple sample processing method has fewer steps than direct water sampling, reducing the potential for contamination during processing.

1.3 Bioindicators and Biomonitoring

Bioaccumulating organisms are often used as an environmental monitoring matrix, most directly expressing the impact of the current ecological status on biota. Organisms which bioaccumulate effectively and proportionally in response to contamination in the water column may be selected as bioindicator organisms.[58] Physiological, behavioural, and biochemical alterations in these organisms, as well as their presence or absence in a given location, are indicative of changes in environmental status.[59] Under the WFD, the monitoring of several organisms as quality elements (such as fish, phytoplankton, and macrophytes) is essential for determining the ecological status of a site.[10] This can be performed visually, for example by inspection of the size of a seagrass bed,[60] or by observing physical alterations of phytoplankton under Scanning Electron Microscopy (SEM).[61]

Assessment of contaminant concentration in an organism's tissues, on the other hand, is known as biomonitoring. Sampling of biomonitor species allows for greater accuracy over direct water sampling when assessing environmental status due to time-weighted averaging of contaminant concentrations the organism is exposed to.[2] When efficient bioaccumulator species are selected for biomonitoring, the concentrations in the organism's tissues can exceed the surrounding waters by orders of magnitude. Biomonitoring also more accurately represents the fraction of contaminants available to biota (the bioavailable fraction), which can be more relevant than total concentrations in waterways when assessing trace metal ecological impact.[23]

However, it is critical to note that many species differ in their response to, and uptake of, trace metals. Macroalgae not in direct contact with sediment accumulate dissolved metals from the water column only, filter-feeding invertebrates can accumulate suspended particulate or particle-bound metals as well as dissolved metals,[59] and rooted macrophytes such as seagrasses can accumulate metals from both the water column and the sediment.[14] In addition, the interaction of coexisting metals at a given

location can influence uptake.[62] As such, a thorough biomonitoring program requires the consideration of more than one biomonitor organism as an analytical matrix, as even closely related species can exhibit different accumulation patterns and biological processes. Studies have been conducted highlighting the variation in metal update between organisms; for example, Søndergaard *et al.* transplanted macroalgae and invertebrates alongside passive sampling devices and noted variations in trace metal uptake potential over 9 days.[63]

The bioavailability of trace metals to biota depends primarily on the speciation of metals in question. The most bioavailable metal species are labile species, which can readily dissociate into free ions or biologically active complexes and be internalised by biota. In the case of free ions, the Free Ion Activity Model (FIAM) and the Biotic Ligand Model (BLM) describe the process of internalisation of trace metals. Following adsorption of a metal to a cellular surface, complexation may occur with a cell feature such as metal transporter proteins, facilitating internalisation of the metal.[43] FIAM and BLM assume that there is an equilibrium between metals adsorbed to the cell surface and metals in the bulk solution, and predicts uptake rates.[46] However, such models may be difficult to apply to the complicated matrix of environmental waters, where there are diverse complexed and adsorbed metal species, and fewer free ions.[43]

Some metals, such as Cd and Zn, form weak complexes in environmental waters,[64] and may be more bioavailable, and complexes formed with Cl^- anions (predominant in seawater) are often toxic due to their solubility in water.[8,40] Certain metal complexes may also permeate the cell membranes via pathways not described by FIAM or BLM. Lipophilic compounds, such as metal-dithiocarbamate complexes, passively diffuse through the cell membrane and form complexes following entry into the cytosol.[43] Complexes formed with inorganic and organic ligands corresponding with cell surface receptors, such as the thiosulphate receptors of the green algae *Chlamydomonas reinhardtii*, may also be readily internalised.[43]

Rainbow defines an ideal biomonitor organism as an identifiable and easily sampled sedentary species present in waterways year-round, which is tolerant of environmental stresses and changes in physico-chemical parameters.[59] These criteria are fulfilled by marine macrophyta such as macroalgae and perennial seagrasses, as

well as sessile invertebrates such as mussels, sponges, and barnacles. Other more motile organisms such as fish are occasionally used as biomonitor species. However, wild species of fish may not be a reliable indicator of the localised environment in which they are sampled, as they may have migrated from sites with differing ecological statuses. Studies on motile organisms are best performed under aquaculture conditions or on transplanted individuals deployed in a restrictive structure to ensure accuracy.

The principles of biomonitoring and bioindicator evaluation are critical in determining overall ecological status of a site. By performing studies which consider speciation, population health, and direct contaminant accumulation of wild species, a more complete assessment of ecological risk is obtained, and such evaluations are essential before undertaking remediation activities. The following sections will focus on select commonly used biomonitor organisms, and their advantages and disadvantages as an assessment matrix of ecological status.

1.3.1 Aquatic Invertebrate Biomonitors

Aquatic invertebrate biomonitors are commonly used in routine temporal and spatial environmental monitoring, and are globally distributed across both freshwater and marine bodies of water.[27] Many invertebrates are filter feeders, siphoning water to consume organic matter and planktonic organisms, and will also take in dissolved and suspended nutrients and contaminants.[23,65] Other are deposit feeders, scavenging food from the bottom sediment, and may also ingest contaminated sediment or organic matter.[54] However, alternative uptake patterns occur; for example, filter feeders may be exposed to contaminants bound to resuspended sediment, and deposit feeders may exhibit uptake from the water column at the sediment-water interface (SWI). Common marine invertebrates used for biomonitoring include mussels (particularly of the *Mytilus* and *Perna* genera), oysters, barnacles, and sponges.

Many marine invertebrates are sessile, attaching to a substrate as larvae and growing in one location. As such, many are recommended as biomonitor organisms, with their tissues providing a time-weighted average of trace metal concentration in their locality over extended periods. However, different invertebrates will be at risk of exposure to distinct species of trace metal contaminants. For example, the barnacle

Amphibalanus amphitrite feeds on microscopic levels, and many particulate phases of metals would be too large for the organism to ingest.[59] In addition, certain invertebrates can regulate metals so they are not incorporated into tissues. Many species of mussels regulate Zn and Cu uptake and tissue concentrations of these essential metals are not fully representative of the bioavailable fraction.[66] As with any biomonitor organism, knowledge of the biological processes undertaken by the chosen invertebrate is essential for accurate interpretation of results.

A distinct advantage of the use of aquatic invertebrates as an environmental monitoring matrix is that many can be easily transplanted from controlled aquaculture sites to a site of interest, where they can be exposed *in situ* to contaminants for a defined period.[31] This allows for control of the period of exposure, and organisms taken directly from aquaculture can be used as a blank for the process, which would not be possible when directly sampling wild populations.[31] Biological factors which may vary and influence metal uptake, such as age, size, and sex of the invertebrates, can also be controlled prior to deployment. The utility of invertebrates, particularly bivalves such as mussels and oysters, has resulted in the group being among the most commonly studied biomonitor organisms.

Mussels

Mussels are an abundant family of bivalve invertebrates which colonise freshwater and near-shore saltwater bodies globally. Most mussels are tolerant to change to environmental status, such as fluctuations in salinity, and undertake adaptive processes to survive in heavily contaminated environments.[31] These adaptations have allowed many mussel species to thrive in suboptimal water bodies, and many species are classified as invasive as a result. Species such as the Asian green mussel (*Perna viridis*) and the black striped mussel (*Mytilopsis sallei*) have migrated substantial distances from their endemic regions via attachment to haulage liners.[67] The abundance of mussels globally, their tolerance of contaminated sites, and their bioaccumulation potential has led to widespread use of mussel tissue for trace metal monitoring. Programs such as the US Mussel Watch Project, the Asian-Pacific Mussel Watch, and MYTIAD in the Mediterranean have been developed to monitor contaminants in mussel tissue.[4]

Mussels are filter feeders and the ingestion of many trace metals leads to long-term retention in mussel tissue following well-defined accumulation models.[65] While mussels regulate uptake of essential trace metals such as Zn and Cu, non-essential metals such as Pb and Cd are readily accumulated in their tissues.[66] *Mytilus edulis*, a widespread and commonly-studied biomonitor species, exhibits a concentration factor of 200-300x greater than the surrounding waters in the case of Pb,[68] and mussels quickly accumulate non-essential trace metals when deployed from an uncontaminated aquaculture site.[66] Many of the trace metal contaminants accumulated by mussels are depurated slowly when ecological status improves (however, a fraction of these are depurated rapidly).[68] As such, wild mussel colonies sampled over several years can provide insight into long-term contamination trends.[4,63]

Many biological and physico-chemical factors affect accumulation of trace metals by mussels. Over the course of a year, mussels exhibit fluctuations in body mass due to their spawning cycles, leading to contaminant concentration changes in the soft tissues independent of uptake.[68] Long-term monitoring projects of wild mussels therefore must ensure that sampling takes place during the same seasons annually. Following transplantation, it may take over a year for mussels to reach comparative tissue metal concentrations to local wild populations.[68] In addition, many physico-chemical parameters affect mussel uptake of trace metals, including dissolved organic carbon (DOC), DO, pH and temperature.[66]

While mussels are in many ways a useful biomonitor organism, analysis of their tissues is a laborious process which may introduce error or contamination. Following sampling, trace metals may be present in the digestive tract of the mussel, as sediment bound species or otherwise not bioavailable. A decontamination process must therefore be performed to purge contaminants not accumulated in tissue, for example by immersing the mussel in water under controlled conditions for 24 hours.[4] Mussels also rapidly depurate a fraction of tissue-accumulated metals such as Pb when moved to uncontaminated water, which may lead to underestimation of tissue concentrations if the purge step is prolonged.[68] The process of tissue analysis following purging has many steps (typically involving the separation of soft tissue from the shell, freeze-drying, homogenisation, microwave digestion, and analysis of the eluate), each of

which can potentially lead to contamination. If error is avoided during processing, however, mussels are an ideal biomonitor organism for a number of contaminants.

Sponges

While many shelled invertebrates are sampled similarly, by isolation of soft tissue for analysis, sponges are a unique invertebrate organism which may also be used for monitoring purposes. Consisting of soft tissues and skeletal structures known as spicules, which may be calcareous or siliceous, sponges are abundant and long-living sessile organisms which can tolerate fluctuations in physico-chemical parameters. Sponges are filter feeders, filtering large volumes of water and accumulating trace metals from dissolved and suspended fractions. Sponges can be easily grown from fragments and can be transplanted to new sites as genetic clones, removing genetic variance which would be a factor when transplanting other invertebrates.[69] In addition, transplanting bivalves may potentially cause the introduction of non-native species to new water bodies, which cannot occur with sponges.

In a study conducted by de Mestre *et al*, two species of sponge were sampled at four sites to investigate variation between sponges at each site and overall trace metals uptake.[69] At each specific site, low variation between sponges was noted, while there were significant differences in average trace metal concentration at each site, highlighting the role these species could play as bioaccumulators. However, the author noted the difficulty of working with the *Mycale* genera of sponges, with a necessity to remove algae and bivalves from the sponge. This study found that there was minor variation in contaminant concentration in the tissue type of an individual sponge. Illuminati *et al*. examined differences in the bioaccumulation in soft organic tissue and spicules of Antarctic sponges, comparing results to Mediterranean species.[23] Similarly, the soft sponge tissue with the spicules removed exhibited similar bioaccumulation potential in each species. However, the necessity to separate soft tissue from spicules prior to analysis is a laborious process and a barrier to easy application of sponges as biomonitors. Despite this, the advantages of an easily relocated sessile species are highlighted.

1.3.2 Macrophyte and Macroalgal Biomonitors

Water bodies globally are host to a wide variety of macroscopic plant and algal species, such as seaweeds, seagrasses, and aquatic mosses. Macrophyte and macroalgae health are essential for the overall health of a water body, as primary producers of oxygen and an important source of food and shelter for biota. They are therefore routinely monitored as indicators of water body ecological status.[60] Seagrasses and many algae remain submerged for their entire life cycle and effectively bioaccumulate trace metals and other contaminants, making them ideal biomonitors to represent aquatic environmental status.

The uptake patterns of macrophytes and macroalgae are relatively simple, often only responding to the dissolved fraction of metals in the water column provided they are not in contact with sediment or rooted.[59] As sessile organisms, macrophytes and macroalgae are easily sampled and their tissues average contaminant concentration over time in their localised environment. However, due to the diversity of these biological groupings in terms of both morphology and biochemical regulation processes, it is challenging to compare even closely related species in terms of tissue contaminant concentrations. The ideal macrophyte and macroalgal biomonitors are widespread and well-studied species, such as the seagrass *Posidonia oceanica* and the green algae *Ulva lactuca*.

Research into macroalgae and seagrasses for trace metal analysis is performed globally, but a substantial portion of these studies are based in the Mediterranean. In a review of published literature on trace metals bioaccumulation by seagrasses and macroalgae, Sánchez-Quiles *et al.* found that 49% of the studies fitting the review's selection criteria were performed in the Mediterranean region.[3] As the Mediterranean Sea is an extremely valuable water body economically and from a biodiversity standpoint, and with increasing trends in trace metal pollution from anthropogenic activity, significant research has been conducted in this region regarding monitoring and remediation of trace metal contamination.[70]

Macroalgae

Macroalgae are multicellular algal organisms, commonly referred to as seaweed. As bioindicators, the absence of sensitive macroalgae or the presence of opportunistic

algal species may indicate contamination or eutrophication events.[58,60] A polyphyletic grouping, macroalgae incorporates red (*Rhodophyta*), green (*Chlorophyta*), and brown (*Ochrophyta*) multicellular algae. These subdivisions represent different evolutionary pathways and hence accumulate trace metals and mediate tissue contaminant concentrations in different manners. They also exhibit varying degrees of tolerance to contamination events or changes to physico-chemical parameters in the bulk solution. Generally, provided the macroalgae is not in direct contact with bottom sediment, bioaccumulation of trace metals occurs from the dissolved fraction in the water column as a function of overall surface area.[58]

The variation of accumulation patterns between macroalgal species for different trace metals have been examined in many studies. Sánchez-Quiles *et al.* identified *Ochrophyta* as the most effective accumulators of As, Cd, and cobalt (Co), and green algae such as the freshwater genus *Oedogonium* and the saltwater *species Cladophora albida* readily accumulate Al.[33,44] Macroalgae typically exhibit two uptake pathways of trace metals; certain lipophilic compounds such as $HgCl_2$ are internalised by passive diffusion into cells, while other metal species may complex with negatively charged surface polysaccharides of the macroalgae before internalization. The three main groups of macroalgae produce unique sulphated polysaccharides: fucose-rich polysaccharides such a fucoidans are found in *Ochrophyta*, galactose-rich carrageenans in *Rhodophyta*, and rhamnose- and xylose-rich ulvans in *Chlorophyta* of the *Ulva* genus.[44] As such, uptake of trace metals heavily depends on the surface area, polysaccharide composition, and morphology of the analysed algal species.[58]

One of the main challenges in the use of macroalgae as biomonitor organisms is the correct identification of individual species. In the Mediterranean alone, over 1,100 species of macroalgae have been identified, and many species in the same genus can be difficult to differentiate.[52] *Ulva lactuca* is an effective and well-studied bioaccumulator, but is morphologically similar to other species with in the genus, and to members of *Enteromorpha*.[59,62] Similarly, the *Oedogonium* genus has hundreds of species, many of which do not exhibit clear physiological differences.[71] For successful biomonitoring using macroalgae, certainty is required on the identification of target species and hence those with distinct and unique morphology may be preferred. Once sampled, macroalgae are processed similarly to invertebrates by freeze-drying, homogenization, and microwave digestion before an eluate is analysed. Macroalgae

also require cleaning to ensure that the algal tissue alone is processed; epiphytic communities which may live on its surface can influence results, but this step introduces another opportunity for contamination to occur.

Seagrasses

Seagrasses are a group of marine angiosperms that are distributed along coastlines globally, other than in the Antarctic Ocean, at depths between 0-40 m below sea level.[3] Seagrass beds are an essential feature of some coastlines, providing shelter and food to various biota, and can help prevent sediment resuspension and coastal erosion due to the thick mat-like formations of roots and rhizomes on the seabed.[14] Due to their importance in the marine biosphere, the WFD includes the monitoring of seagrasses and other aquatic angiosperms as one of its biological quality elements.[10,60]

Seagrasses are ideal bioindicator and biomonitor organisms due to their wide geographical distribution, sessile nature, ease of identification and sampling, and extensive and specific bioaccumulation of trace metal contaminants.[2,58] The methodology of using seagrasses as a bioindicator is applied to *Zostera* seagrasses by Wilkes *et al.* [60] As many species of seagrass are tolerant of substantial trace metal concentration in the water column, showing little physical alteration in highly contaminated waters,[52] assessment as a bioindicator is usually based on the prevalence of seagrass beds and the biomass of individual plants.[10,60]

The resistance of seagrasses to trace metal contamination makes the grouping a beneficial sampling vector for trace metals. Seagrasses exhibit two bioaccumulation pathways, accumulating dissolved fraction bioavailable metals directly from the water column as well as from the porewaters of the sediment in which they are rooted.[14] Seagrass tissues can be sampled for a time-weighted average of metal exposure, and different sections of the plant can be used to average different periods of contamination due to the kinetics of uptake and metal mobilization within the plant. In the case of the Mediterranean endemic seagrass *Posidonia oceanica*, the leaves and shoots approximate two weeks of previous exposure,[14] whereas sampling the first centimetre of new rhizome growth can be used to estimate a year of exposure.[34] While seagrass species exhibit varied bioaccumulation potential, and compartmentalize and regulate trace metals differently, in general essential micronutrients follow an uptake

pattern of [Fe] > [Mn] > [Zn] > [Cu], while non-essential metals have no distinct uptake patterns.[72]

The Mediterranean seagrass *P. oceanica* has been studied extensively as a bioindicator and biomonitor organism and is recommended under the WFD as a monitoring element where available.[73] This species is endemic to the Mediterranean coastline at depths between 0-10 m below sea level, and an estimated 2.5 to 4.5 million hectares of coast are covered by *P. oceanica* meadows.[74] The species is hardy in metal-enriched waters, and resists many changes in physico-chemical parameters, but cannot tolerate low salinity.[52,73] The thick mat-like structure of *P. oceanica* meadows, featuring dense canopies of leaves, allow for the effective sequestration of contaminants in the water column and reduces suspended sediment in solution as demonstrated in Figure 1.2. This process limits exposure of contaminants to other organisms and its own young shoots, and *P. oceanica* can effectively accumulate up to 27 different metals and metalloids, initiating this uptake process within hours of exposure.[75]
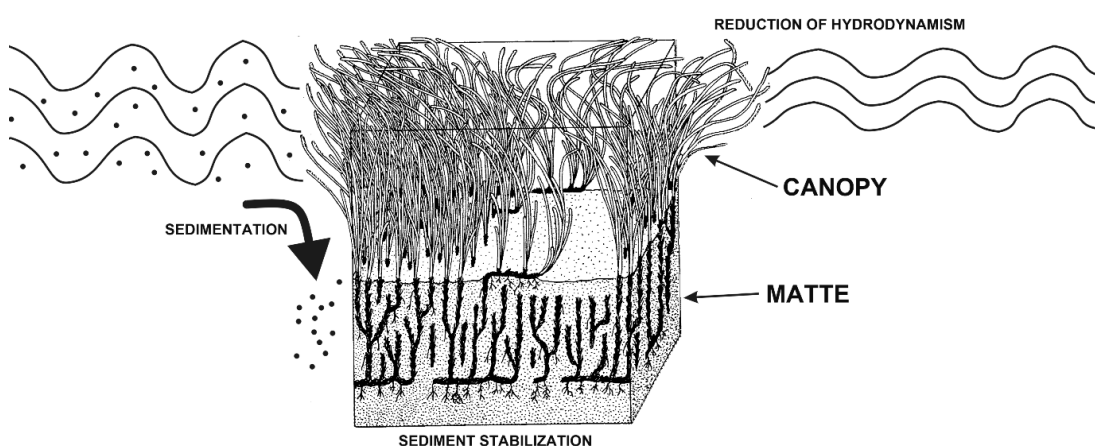
Figure 1.2. Schematic by Boudouresque *et al.* of the sediment trapping and stabilization processes of a *P. oceanica* meadow.[73] Standard hydrodynamics are disrupted by interaction with the thick canopy of seagrass leaves, causing suspended sediment to sink.

In the case of certain non-essential trace metals, such as Cd and Pb, seagrass physiology can impact bioaccumulation potential as diffusion takes place as a function of surface area.[14] The age of leaves also affects accumulation, and larger and older leaves tend to have increased trace metal concentrations in their tissues, with the

exceptions of Cu and Cr.[2] Seasonal variations can result in changes in biochemical processes, and some studies suggest that essential micronutrients such as Cu, Zn and Mn are stored in the rhizomes during winter and translocated to shoots to promote growth during summer months.[14] However, other researchers have observed the inverse, with higher Fe, Zn and Cu concentrations in the leaves of five seagrass species documented by Prange & Dennison in winter months (September – January), correlating with higher rainfall.[19] The seasonal variation patterns in their tissues highlight the requirement of long-term monitoring of trace metal concentrations in each seagrass, as sampling during different periods introduces uncertainty regarding accuracy.

While *P. oceanica* is exclusively found in the Mediterranean region, all seagrasses can be sampled in a similar manner and are efficient bioaccumulators, such as the globally distributed *Zostera* genus.[60] *Zostera* seagrasses effectively accumulate priority metals Pb and Cd, but are also sensitive to high concentrations of Cu, leading to toxic effects. Both *Z. capricorni* and *Halodule uninervis* exhibit decreased amino acid production in Cu-contaminated waters (potentially due to Cu^{2+} attack on thiol groups), while other seagrass species such as *Cymodocea serrulata* appear to regulate internalised Cu concentrations.[19] Regardless of the species, seagrasses all similarly uptake trace metals from both the water column and sediment porewaters and can be used to investigate the impact of contamination events in similar manners.

At present, anthropogenic pressures are one of the most significant causes of seagrass regression, and such species may not always be present in certain regions. Debate surrounds the amplitude of human impact on seagrass meadows, but it is accepted that activities such as aquaculture, shoreline restructure, and trawling have a negative impact on their health.[74,76] Physical removal and decreased salinity due to coastline restructure and changing hydrodynamics directly impacts seagrass health, and eutrophication events due to effluent input may increase water turbidity and impede photosynthesis of the underlying meadow. Concern has also been raised regarding the impact of climate changes on these meadows, with researchers indicating increased water temperatures have resulted in heightened mortality for young seagrass shoots. For example, researchers such as Jordà *et al.* predict the functional extinction of *P. oceanica* by 2050 due to the mortality of new growth.[77] The increased scarcity in areas of anthropogenic pressure highlights the necessity for alternative methods of trace

element monitoring, as absence of well-studied biomonitors in contaminated water bodies further complicates accurate monitoring of environmental impact.

1.4 Passive Sampling Devices (PSDs) for Environmental Monitoring

The trace metal monitoring methods of water, sediment, and biomonitor sampling described above are useful tools in evaluating the ecological status of a water body. However, each method has limitations which may make interpretation of results challenging. In water sampling, the lack of time integration, outside of laborious and frequent sampling, provides point trace metal concentrations only and is not indicative of ecological status over extended periods. Sediment sampling provides this time integration, but does not provide reliable information regarding bioavailability, as the binding capacity of sediment depends on organic matter content. Sediment deposited trace metals will also be subject to speciation changes due to biological activity and localised fluctuations of physico-chemical parameters. While biota sampling is clearly indicative of the direct impact of trace metals on organisms in the environment, due to different uptake pathways and regulation of tissue metal concentrations, it is difficult to extrapolate findings outside of direct impact on the given organism. Given heightened concerns regarding the impact of climate change on mortality rates of some common biomonitors, alternative methods may need to be explored.

Passive sampling devices (PSDs) have seen increased use as an alternative to traditional sampling methods for many contaminants. These devices allow for the continuous accumulation of a contaminant of interest over time and follow well-defined uptake patterns.[37] Factors which affect some of the other discussed sampling methods, such as DOM content in sediment and water, and regulation methods by biota, are often negligible when using PSDs. PSDs can be introduced to waters of any ecological status, even where there may be few native bioaccumulators or where transplanted bioaccumulators may not survive. Some devices are also thought to be representative of the dissolved bioavailable fraction only.

While not currently accepted as a monitoring tool under the latest revision of the WFD (Directive 2013/39/EU), they are mentioned in Article 18 as *"…show[ing] promise*

for future application, and their development should therefore be pursued."[11] The ease of use and analysis, and the low cost of many PSDs is of particular advantage in the implementation of regulatory policy, reducing the financial burden on laboratories undertaking such monitoring programs. Reduced start-up cost for regulatory monitoring laboratories, as well as robust protocols for their use and analysis, helps achieve of the aims of the WFD. For the purposes of passive sampling of trace metals in solutions, one of the most widely studied devices is the Diffusive Gradients in Thin Films (DGT) device.

1.4.1 Diffusive Gradients in Thin Films (DGT) Devices

DGT passive sampling devices are an effective means of measuring contaminant concentrations in solution. DGTs consist of a binding layer which retains analytes of interest, separated from the bulk solution by a diffusive gel layer which allows effectively unimpeded diffusion of analytes through the device.[78] A membrane filter is usually also incorporated to prevent particles clogging the diffusive gel. A diagram of a standard DGT assembly is illustrated in Figure 1.3. DGTs have been applied *in situ* to monitor a wide range of contaminants in ground porewaters, marine waters, and freshwater rivers and lakes, due to its simplicity of design and well-defined characteristics.[38,41,57,78]
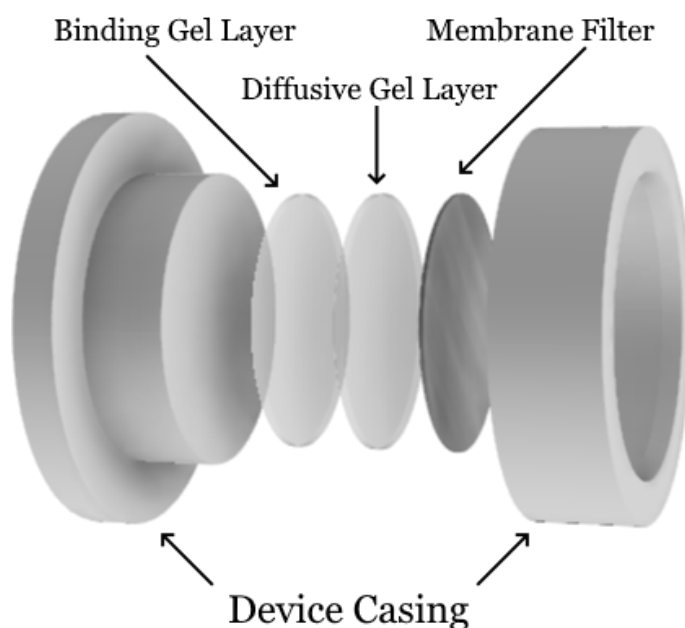
Figure 1.3. Exploded-view diagram of a standard DGT device assemblage.

DGTs are a beneficial monitoring tool as they effectively pre-concentrate analytes *in situ*, eliminate matrix effects of the bulk solution, and allow for quantitative measurement of some analytes to concentrations as low as 4×10^{-12} mol/L.[78,79] Within the diffusive layer of the device, mass transport is limited to simple diffusion in accordance with Fick's First Law, which states that flux due to diffusion is proportional to a concentration gradient. DGT measurements are converted from flux (μg cm^{-2} s^{-1}) to bulk solution concentration (μg/L) by a series of calculations based on this Law, as presented by Zhang & Davison and other researchers.[78] As analytes diffuse through the device, a concentration gradient is formed, as seen in Figure 1.4.
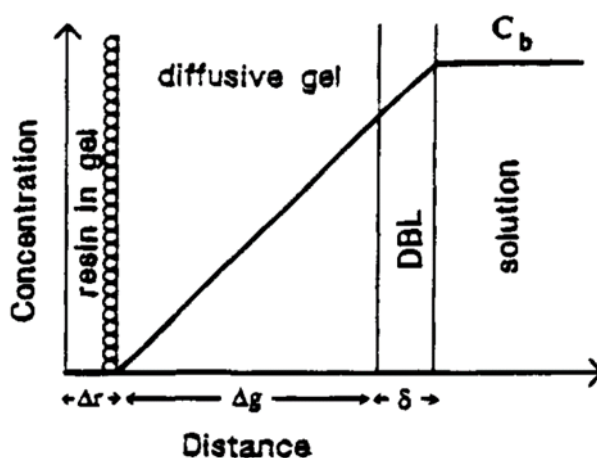
Figure 1.4. Diagram of the concentration (C_b) of an analyte in relation to distance diffused through the diffusive gel (Δg), reproduced from Zhang & Davison.[78] The diffusive boundary layer (DBL), a theoretical boundary in which there is no flow, may be considered an extension (δ) of the diffusive gel in solutions of low flow.

A wide range of analytes can be accumulated by DGT devices by selecting an appropriate binding layer.[64] For trace metal monitoring, the Chelex 100 chelating resin is the most common binding layer due to its strong and specific binding of metal ions. The diffusive gel used in this standard device is an agarose crosslinked polyacrylamide (APA) gel. Chelex 100 binding layer DGTs can accumulate free ions and weakly complexed metals such as chlorides, hydroxides, carbonates, and sulphides, provided they are smaller than the pore size of the APA diffusive gel (typically 9 nm diameter).[37,41,64] The strength of Chelex 100 as a chelation agent induces some of these weak complexes to dissociate, resulting in binding with the resin.[41,78]

Physicochemical parameters which primarily affect DGT trace metal uptake include temperature, pH, and salinity or ionic strength of a solution. Of these factors, temperature is critical as the diffusion coefficients for metals in the APA diffusive gel change with respect to temperature, as shown in Figure 1.5. Temperatures outside a range of ±2 °C over the course a deployment are suboptimal for accurate quantitation as a result. The pH of a solution also affects DGT uptake of trace metals, changing metal speciation and affecting binding efficiency of the Chelex 100 resin, which has an optimal pH range of 5 – 8.3. Typically, natural waters have a pH between the range of 4 – 9, but in waters such as industrial effluent receiving waters poor binding of metals by Chelex 100 may occur. Ionic strength and salinity can also affect diffusion, with high salinity reducing diffusion by up to 8%.[50,78]
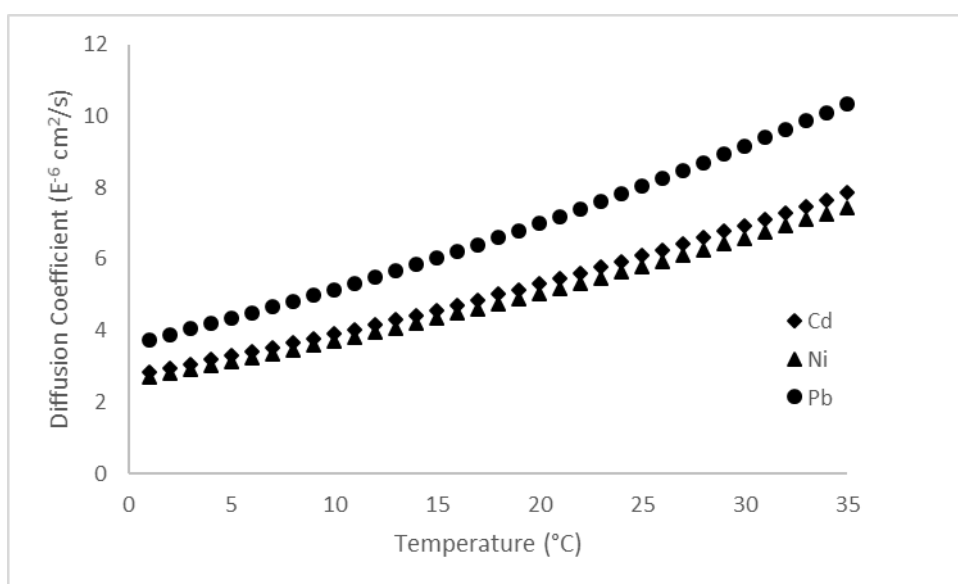
Figure 1.5. Change in diffusion coefficients of Water Framework Directive priority metals in APA diffusive gel in response to temperature variation. Data obtained from DGT Research Ltd.[80]

The fraction of metals measured by DGT is commonly referred to as the DGT-labile fraction and is assumed to approximate the bioavailable metal fraction by many researchers. DGTs have been used in many studies under this assumption.[33,57,75] Theoretically, under the FIAM (as discussed in Section 1.3), bioavailable and labile fractions should be equivalent, but there are difficulties relating the concentrations measured by DGT directly to biota tissue concentrations. As described previously, many organisms differ in bioaccumulation patterns, but DGT also interacts with some

metal species during deployment. For example, Chelex 100 binding resin causes dissociation of some weakly bound complexes, and in low ionic strength solutions the APA diffusive gel may exhibit some retention of species such as Cd free ions.[41,64] Nevertheless, as will be discussed in more detail below, concentrations measured by DGT have been shown across many studies to be a more accurate predictor of bioavailability than total dissolved concentrations.[41]

Under ideal conditions, diffusion occurs across the thickness of the diffusive gel (Δg in Figure 1.4) only, but a number of factors may ultimately affect the distance from the bulk solution to the binding resin. Under certain circumstances, the diffusive boundary layer (DBL) must be considered an extension of the diffusive pathway length in calculations, particularly in experimental setups with low flow rates.[78] The DBL is a theoretical boundary between a solid surface and a solution in which it is submerged in which the kinetics of analyte uptake are controlled by diffusion only and there is, in effect, no rate of flow. Its thickness is inversely proportional to the flow rate of a solution and above a threshold level of flow, the DBL is negligibly small above the DGT surface and can be excluded from calculation. In environmental monitoring, most water bodies including lakes exhibit flow rates above this threshold, and the impact of this factor on deployed DGTs is limited.

A common limitation of deployments in environmental waters is the presence of a wide range of organisms which may readily adhere to a surface and proliferate in a process known as biofouling. Biofouling was noted as a potential limiting factor of the DGT device since its inception,[79] and a developed biofilm community can bind metals and change their speciation, preventing binding by the device. In addition, the formation of a film incorporating extracellular polymers and insoluble particles impedes diffusion, increases the distance to the binding layer, and may clog the pores of the DGT. A more detailed examination of the processes and challenges of biofouling in the context of DGTs will be discussed in Chapter 2. In short, the difficulty in reducing biofouling *in situ* means that the deployment time of DGTs for accurate quantitation is limited by the proliferation of fouling organisms on the device surface. Some methods allow for long-term deployment of the devices, such as the THOЁ apparatus which includes a programmable sample carousel, mitigating the effects of biofouling by exposing the devices for shorter periods.

DGT devices are easily analysed with a reduction in handling when compared to laborious biomonitor analysis processes, reducing the risk of sample contamination. Extraction of trace metals from biomonitor tissue often requires steps including the manual isolation of desired tissue, freeze-drying, homogenisation, and microwave digestion prior to analysis of the eluate. In contrast, DGT devices are opened, the binding resin is removed, and trace metals are subsequently extracted from the resin by immersion in 1 M nitric acid for 24 hours prior to analysis. This simple method of extraction also reduces the upfront costs for a laboratory undertaking monitoring programs, as no specialised apparatus is required other than analytical instrumentation such as ICP or stripping voltammetry.

DGT devices may be applied as an alternative to the biomonitors described in previous sections, as their ease of deployment and well-documented characteristics eliminate many variables which may be encountered when sampling biota. The DGT devices may be deployed year-round, and data from each deployment is comparable, which may not always be the case for biomonitor organisms which undergo seasonal fluctuations in total tissue mass. A number of comparative studies have been conducted investigating the relationship between DGT accumulation and concentration in tissues of chosen biota.[81] The following section will examine this relationship for a select number of commonly used bioindicator organisms.

1.4.2 DGT Trace Metal Accumulation Versus Bioaccumulation

DGT Accumulation Versus Macrophyte Bioaccumulation

In terrestrial plants, DGTs have been extensively studied as a predictor of uptake of trace metals via the roots from soil.[57] Effectiveness of the predictive technique varies; DGTs are poor predictors of Zn in grasses and lettuces, but effectively predict Cd uptake in wheat and maize.[57] Comparative studies between trace metals in aquatic plants and DGT devices have been conducted less frequently, and many in this area focus on the uptake of the essential mineral phosphorous.[82–84] However, a number of researchers have researched select macrophyte bioaccumulators and DGT-labile trace metals.

Schintu *et al.* explored the relationship between concentrations of four metals measured by DGT and the tissues of *Enteromorpha* sp. and *Padina pavonica* (L.)

Thivy algae at five sampling sites.[62] As *Enteromorpha* was difficult to identify when compared to other green algae, emphasis is placed on the uniquely structured and easily identifiable *P. pavonica*. Statistically significant relationships between DGT accumulation and *P. pavonica* Pb and Cd uptake ($p < 0.05$) occurred at all sampling sites studied, while Cu measurements between the sampling methods had no strong correlation. Zn, which was measured by DGT, was not compared to macroalgae. Similarly, Søndergaard *et al.* noted strong correlations between DGT-labile Pb and Zn and tissues of growth tips of transplanted *Fucus vesiculosus* after nine days of deployment ($R^2 = 0.87$ & 0.82 for Pb and Zn, respectively). However, poor correlation was observed in the case of Fe, suggesting the regulation of Fe by the seaweed even during short deployments.

Comparative studies between DGT-labile metals and aquatic mosses are currently limited. Diviš *et al.* studied trace metal uptake by the freshwater moss *Fontinalis antipyretica*, comparing to DGT-labile and total dissolved metals.[85] Correlations between DGT-labile Pb and Zn and moss tissue were stronger than with total dissolved metals, while the inverse was exhibited in the case of Cu and Ni. *Fontinalis antipyretica* and other aquatic mosses uptake both labile Cu and more strongly complexed species, indicated by the stronger correlations to total dissolved Cu. However, further study of correlation between DGT-labile metals and other aquatic mosses are needed to fully interpret these findings.

Macrophytes with a developed root system, such as seagrasses, complicate correlation studies with DGT-labile trace metals due to their trace metal uptake from both sediment porewaters and the surrounding bulk solution. These accumulation patterns vary for differing metals and seagrasses, further making comparisons challenging; for example, Cr, Hg and Ni concentrations in *P. oceanica* shoots are closely related to sediment concentrations of these metals.[53] The DGT Induced Fluxes in Sediment model (DIFS) is used to predict the kinetics of trace metal uptake from sediment porewaters.[86] Wang *et al.* demonstrated that correlations between DGT-labile concentrations and root tissue concentrations in *Zizania latifolia* and *Myriophyllum verticillatum* were greater than correlations between root and total sediment concentrations of Cu, Zn, Pb and Cd.[86]

Other studies on seagrasses have attempted to relate trace metal concentrations in the whole plants to sediment porewater concentrations; Kilminster compared the leaf and root tissues of *Halophila ovalis* and *Ruppia megacarpa* to DGT porewater measurements at several depths, and found slight correlations ($R^2 = 0.51$) between the two methods overall at depths of 9-12 cm subsurface.[72] The strongest relationship was found to be between sediment trace metals extractable by HCl and the seagrass tissue concentration, which indicates potential difficulties in direct *in situ* comparison between DGT accumulation and seagrass uptake. At present, comparative studies are limited for rooted macrophytes, and commonly used biomonitor species such as the *Zostera* genus and *P. oceanica* have yet to be by this method, despite DGT being used to estimate the bioavailable fraction to these seagrasses in some studies.[75]

DGT Accumulation Verses Invertebrate Uptake

As invertebrates such as mussels are routinely used for monitoring programs, many studies have been conducted to relate mussel tissue concentrations to DGT-labile trace metals. Schintu *et al.* transplanted *Mytilus galloprovincialis* from a controlled aquaculture site to four coastal Sardinian sites in tandem with DGT to monitor four metals.[87] Significant correlations ($p < 0.05$) were determined between Cd and Pb mussel tissue accumulated metals and DGT-labile concentrations, with no evidence of correlation noted for Cu and Ni. Søndergaard *et al.* similarly found strong correlations ($R^2 = 0.88$) between DGT-labile Pb and *M. edulis* tissue concentrations.[63] This supports previous studies suggesting that mussels effectively regulate Cu but continue to accumulate Pb.[66]

DGT devices have also been co-deployed with sediment-dwelling deposit feeder invertebrates, such as *Tellina deltoidalis*. Simpson *et al.* observed strong correlations between flux of Cu into DGT devices at the SWI and the tissue concentration of *T. deltoidalis* ($R^2 = 0,87$).[56] However, correlation between the organism's tissue concentrations and the total concentration of time-averaged overlying waters was stronger. The authors suggest that the short-term study, involving artificial contamination of sediments with Cu in a controlled laboratory setting, may not accurately represent conditions *in situ* in the environment. Further studies conducted by Amato *et al.* suggest that this organism may partially regulate Zn, but above a concentration threshold DGT accumulation of Zn and *T. deltoidalis* tissue concentrations were strongly correlated.[54]

As invertebrate biomonitors are a diverse grouping, some studies have found that certain organisms do not respond to the DGT-labile fraction of metals. For instance, tissue concentrations of the yellow lampmussel (*Lampsilis cariosa*) did not correlate with the DGT-labile fraction of Cu and Pb.[5] Other research by Vannuci-Silva *et al.* using transplanted *Nodipecten nodosus* scallops noted evidence of accumulation of Cd prior to transplantation. These studies, while negative, highlight the value DGT devices may present for the assessment of water quality, as transplanted organisms carry a background level of contamination which may impact on results, or chosen biomonitors may be poor accumulators of certain labile metal species.

DGT Accumulation Versus Uptake by Other Aquatic Organisms

As demonstrated in the preceding sections, equating DGT to individual biomonitor species directly can be challenging. The varying bioaccumulation potential of organisms and the differences in biochemical response to these ecological stressors means that in many cases biomonitor species do not directly indicate bioavailable metals at a given location. Findings across a number of studies suggest that there are difficulties in using DGT-labile Cu as a predictor of accumulation in tissues of living organisms, but the prediction of bioaccumulation of non-essential metals such as Pb is more accurate.[62,66,85,87] However, there are certain organisms which contrast this finding; Cu accumulation in fish gills such as those of the rainbow trout and fathead minnow is more accurately predicted by DGT (R^2 = 0.8 and 0.69 respectively, p < 0.05).[5,88] Previous studies suggest that the gill tissue concentrations of the fathead minnow correlate with free Cu^{2+} in solution, a fraction that would be DGT-labile.[89]

One group of organisms which may be useful in evaluating the correlation between DGT-labile metals and the bioavailable fraction are phytoplankton such as diatoms. Phytoplankton accumulate trace metals directly from the dissolved phase only and are not influenced by colloidal forms.[90] These short-lived organisms, which only survive for a few days, allow for short-term averaging of contaminants in their environment. This rapid mortality means that the overall planktonic community rapidly changes in response to ecological stressors, resulting in dominance by resistant species. Hardy species such as *Achnanthidium minutissimum* may replace more sensitive diatom genera such as *Cocconeis* and *Cymbella* following contamination events.[61] As an

organism on the lowest trophic level, analysis of bulk phytoplankton cellular content can provide insight into biomagnification potential if used as a food source by other organisms.

Phytoplankton require a base level of micronutrients for optimal growth such as Cu, Fe, and Co, and it is suggested that low concentrations of these nutrients in labile forms could be a limiting factor of diatom growth and proliferation.[91] Under controlled conditions, the uptake of trace metals by phytoplankton should follow the FIAM of bioavailability, and hence their cellular metal contents should correlate with DGT uptake.[81] The Arctic diatom *Attheya septentrionalis* exhibits this, with strong positive correlations between DGT-labile Cd and V and intracellular concentrations under laboratory conditions ($R^2 > 0.99$).[90] Field tests using this diatom also found positive correlations (at lowest, $R^2 = 0.84$ and 0.79 for Cd and V respectively). These findings agree with earlier work by Bradac *et al.* indicating strong correlation between intracellular Cd of a wild phytoplankton community and DGT-labile Cd ($R^2 = 0.91$).[46] At present, there is limited comparison between these two methods, for a very small number of non-essential metals. Further study of the correlations between phytoplankton cellular contents and DGT labile metals is required before drawing definitive conclusions on this relationship, but it is a promising method of evaluating the assumption that DGT devices measure the bioavailable fraction of metals.

1.5 Summary

The monitoring of trace metal concentrations in water bodies to determine overall ecological status can be performed using many different methods, each with benefits and challenges. As demonstrated, biomonitor organisms are particularly advantageous due to their prolonged exposure to the environment and to contaminants of biological concern, providing time-integrated assessments of the water body's ecological status. However, due to variance of metal uptake and regulation by organisms, it is often challenging to determine the impact of contamination events on the wider ecological community of the water body from the tissue concentrations of a small number of biomonitors.

The use of PSDs such as the DGT device offers more insight into the chemical speciation of metals in both bulk solution and sediment porewaters. As the DGT

device measures a labile fraction of metals, comprising free ions and weak complexes which are assumed to be bioavailable under the FIAM, there is potential for the DGT device to be used in place of biomonitor organisms for ecological status evaluation. However, as demonstrated in this review, bioaccumulator organisms respond to different fractions of dissolved and particulate metals due to various biological processes. The use of DGT or similar PSDs offers a well-defined standardized sampling matrix which can be employed across broad geographical areas or intermittently over long periods, reducing variance when compared to sampling of various biomonitor organisms.

Due to the DGT's status as a cheap, robust, and easy to analyse tool for the evaluation of the chemical status of waters, it may be applicable to a wide range of monitoring programs following studies to develop EQS for priority metals in DGT. The method has yet to be approved for use under the WFD as of the latest revision, and there is a need to further evaluate the bioavailable of the DGT-labile fraction for a larger range of metals, including the priority metal Ni which is most studies was not examined. Pending further research, the DGT device may simplify the monitoring of ecological status by reducing laborious sampling and minimizing risks of contamination during sampling processing, as well as eliminating the variance introduced by using biomonitor organisms as a sampling matrix.

This thesis aims to further progress trace metal monitoring and analytical methods. As biofouling is a commonly reported limitation of DGT PSDs, the examination of biofouling development on the device's surface, such as incidence, speciation, and comparison to water parameters is considered. The stripping voltammetry analytical technique is also examined, presenting a low-cost method for trace metal analysis in solution. Here, SV methods are adapted to optimize the analysis of low concentrations of the WFD priority metals (Pb, Ni, and Cd). Taken together, these findings aim to inform future trace metal monitoring programs.

Chapter 2

Impact of Biofouling on Passive Sampling Devices and Examination of Fouling Environments of Atlantic and Mediterranean Waterways

2.1 Introduction

Biofouling is the colonisation and proliferation by undesirable organisms on a surface immersed in an environmental medium.[92] In environmental waters, microscopic (bacteria, microalgae, fungi, etc.) and macroscopic (macroalgae, mussels, barnacles, etc.) organisms can constitute a biofouling community. In the case of many industrial operations and environmental monitoring programs, biofouling poses a significant threat to successful operations, and its mitigation or prevention is critical.

In aquatic environments, the traditional model of biofouling starts with the buildup of dissolved organic matter on the surface of an object, as illustrated in the first step of Figure 2.1.[93] The organic matter forms a conditioning layer, modifying the roughness and physico-chemical properties of a surface.[94,95] The nutrient-enriched environment of the conditioned surface promotes attachment of microbial fouling species (step 2 of Figure 2.1).[96] Larger secondary fouling microorganisms then begin to colonise the surface. Adhered microorganisms immobilise themselves by secreting extracellular polymeric substances (EPS), and the layer formed by EPS, microorganisms, and other incorporated particles is known as a biofilm. A developed biofilm increases mechanical stability of fouling organism, protects against desiccation, and promotes the absorption of organic material from water.[97] The surface physico-chemical parameters are also further modified by biofilm development, promoting further colonisation of the surface in subsequent days and weeks, forming a more complex fouling community including macroscopic multicellular organisms.
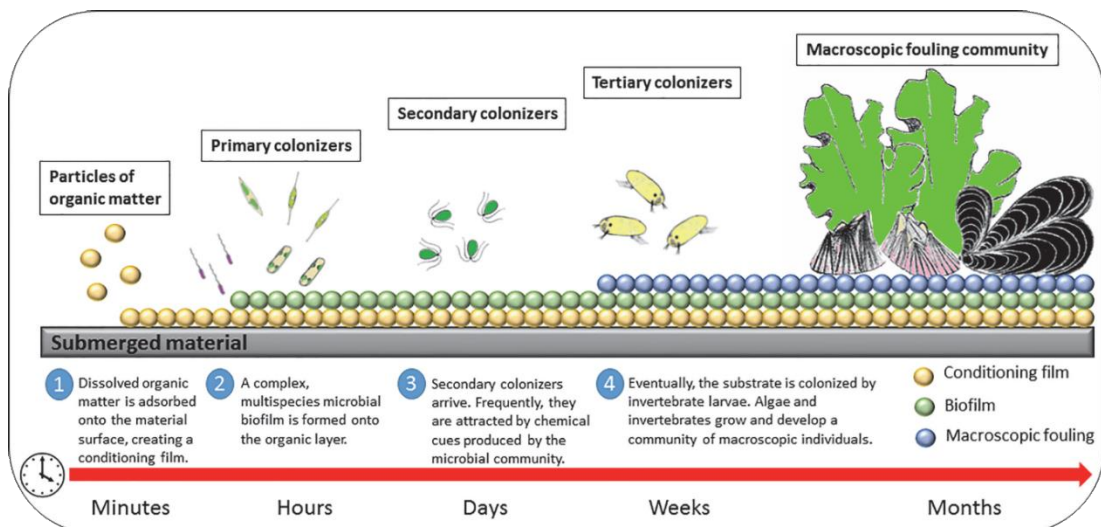
Figure 2.1. A schematic representation of the traditional model of biofouling, with examples of adhering organism types at each stage.[98]

In addition to this generally accepted process of biofouling, organisms can settle on surfaces without prior development of a conditioning film. For example, in a study by Callow *et al.*, microalgal *Enteromorpha* zoospores could adhere directly to clean glass surfaces within minutes.[99] Barnacle larvae have similarly been found to attach to clean glass surfaces as soon as 24 hours after immersion,[100] but it has been demonstrated that a developed biofilm promotes larval settlement on glass, while inhibiting settlement on polystyrene.[101]

Depending on the fouling species settled on a substrate, and the nature of the EPS secreted (as it is a complex mix of protein and carbohydrate constituents), biofilms can develop in an unpredictable manner and form a random-three dimensional structure which incorporates organic matter and particulates. As such, every incidence of biofouling is unique, as the buildup is not uniform and the biodiversity of fouling on any given surface is influenced by a number of factors.[102]

One common group of fouling microorganisms are diatoms (members of the *Bacillariophyceae* class). Members of this phylum of unicellular algae are present in almost all aquatic environments.[103] Diatoms are one of the most significant groups of primary producers of oxygen, contributing to an estimated 20% of total global production.[104] They are notable for their distinct silica outer shell, known as a frustule, which is highly ornamented and unique for every studied diatom genus. These frustules express a form of symmetry, either bilateral (known as pennate diatoms) or radial (centric diatoms). Examples of both pennate and centric diatoms found in marine sediment are included in Figure 2.2. Due to these characteristics, determination of a diatom to genus level can be performed solely visually through identification of key features of frustule structure. However, it is important to note that diatoms may undergo frustule deformations as a result of environmental stressors, which may make identification via this method challenging in some cases.[61]

There are approximately 160 genera of diatoms found naturally in marine waters.[105] In traditional models of biofouling, diatoms adhere to a surface following conditioning by bacterial EPS secretion, generally within the first few days of immersion. However, certain species of diatoms can readily adhere to antifouling surfaces which other microorganisms cannot easily inhabit. For example, silicon-

based fouling release coatings, which have a low surface energy and allow for easy removal of many fouling organisms, may not impede the settlement and proliferation of diatom slimes.[106] Similar to bacteria, diatoms excrete forms of EPS which allow for movement along substrates, improve sessile attachment to surfaces,[107] and promote colony formation.[108] These secretions can form a conditioning film and promote attachment of further fouling organisms, meaning that diatoms can facilitate fouling on certain surfaces that resist traditional early foulers. Diatoms from eight genera are mostly associated with fouling, and other genera can contribute to these biofouling communities but are generally less prevalent.[107] However, as the distribution of diatom species varies geographically, different diatoms will dominate fouling in different regions.[109]
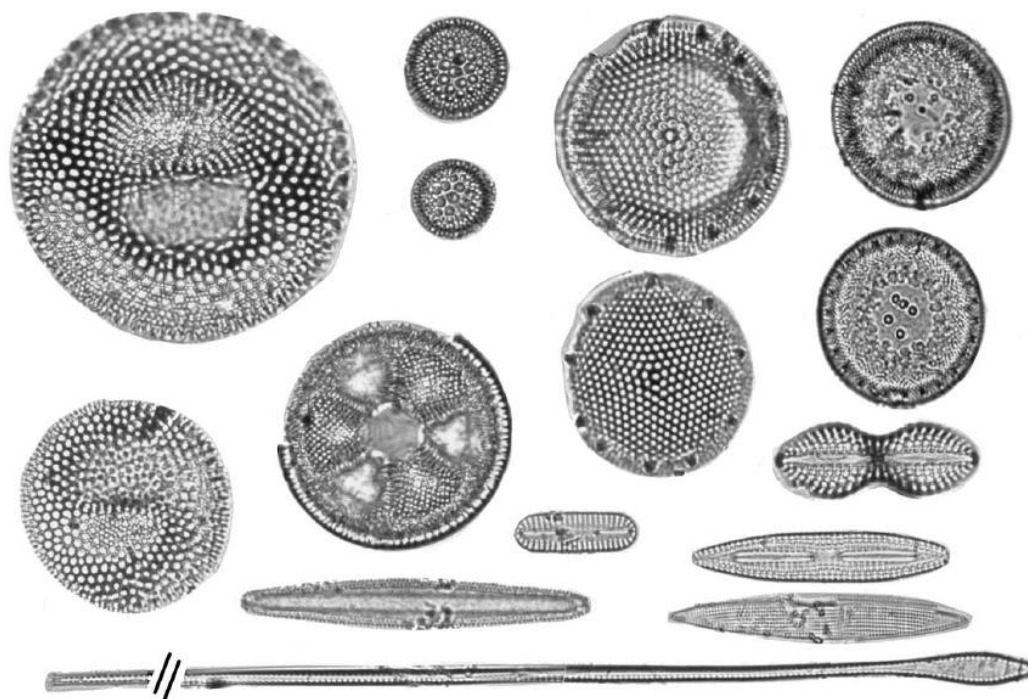
Figure 2.2. Examples of centric (top) and pennate (bottom) diatoms, found in sediment cores taken in the Atlantic area of the Southern Ocean. Adapted from Censarek & Gersondel.[110]

Medium to long-term environmental monitoring programs can be made significantly more difficult due to biofouling. Buildup of a biofilm on the window of an optical sensor, for example, results in light being blocked partially, and eventually completely, by translucent and opaque biofilm constituents.[111] Other forms of sensors can be impacted due to the metabolic activity and irregular shape of the biofilm, which

can form small channels within. These factors may lead to localised changes in physico-chemical parameters such as pH, dissolved oxygen, and conductivity, which may not be representative of the bulk solution beyond the biofilm.[112] These conditions generate substantial noise and error in measurements.

Due to the heterogeneity of biofilms in both morphology and biodiversity, it is nearly impossible to predict how measurements will be impacted by fouling. Kerr *et al.* demonstrated that the impact of biofouling on the measurements by two optical sensors followed a non-linear pattern.[111] Transmissometer readings had a clear critical point (t = 150 h) after which fouling buildup resulted in the loss of data. However, the other deployed instrument, a fluorometer for chlorophyll-α measurement, experienced more complex disruption patterns; increased fouling caused an increase in chlorophyll-α measurements when fouling levels were low, but this impact was lessened at higher concentrations of chlorophyll-α in solution. Diversity of fouling, again, may cause these results, with a biofilm rich in algae and photosynthetic bacteria being a probable cause of spikes in chlorophyll-α measurement.

Due to the variability of biofouling in terms of its components, rate of accumulation, and impact, it is clear that a preventative approach is favourable over attempting to account for its effects on measurements. Following the global ban of TBT biocidal paints due to the toxicity of the chemical to non-target organisms,[28] methods to combat fouling have diversified significantly, as discussed in reviews such as by Whelan & Regan.[113] Methods include the incorporation of copper-based biocidal paints into the design of an instrument,[114] use of automated brushes or chlorine jets to clean surfaces,[115] and use of modified surface coatings, which can prevent initial settlement or allow for easier removal of developed biofouling.[116]

Passive sampling devices are similarly affected by biofouling. One commonly used PSD, particularly for the analysis of trace metals, is the Diffusive Gradients in Thin Films device. The standard design of a DGT device allows for the accumulation of trace metals from solution to provide a time-weighted average of labile metal concentrations, using well-defined diffusive characteristics of metals.[78] A developed biofilm on a DGT's surface affects the free flow of metals from bulk solution to the

device, impacting measurement. Biofouling was identified as a challenge to successful DGT deployments in the initial design of the device, and as an unpredictable environmental parameter, mitigation of fouling is essential.

The formation of a biofilm on the surface of a DGT device results in a number of changes to the system, and in one study led to a two- to three-fold decrease in accumulated trace metal concentrations compared to clean devices.[117] A developed biofilm adds to the overall thickness of the device, and the biofilm itself has an unknown diffusion coefficient to a given metal. Thickness of device elements between the bulk solution and the binding resin is a component of the conversion of metal flux into the device ($\mu g\ cm^{-2}\ s^{-1}$) to overall bulk solution concentration ($\mu g/L$). Therefore, thickness added by a biofilm may need to be considered in calculations, as demonstrated in Figure 2.3. However, this is debated; Feng *et al.* proposed a series of equations to include biofilm thickness and diffusive properties into account, while other researchers such as Uher *et al.* modelled the kinetics without an increase in the material diffusive layer thickness.
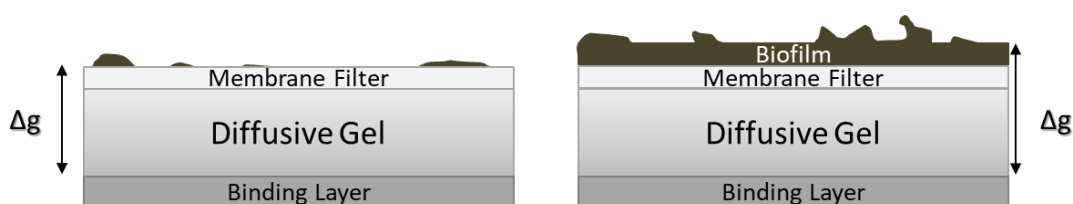
Figure 2.3. Schematic of development of a biofilm on a DGT device, affecting free flow of labile metals and potentially increasing the distance (Δg) between the binding layer and the bulk solution.

While labile metals diffuse through the hydrogel layer relatively unimpeded, due to its diffusive properties being similar to water, the effects of a biofilm on diffusion would be unknown and would depend upon composition and local environmental factors. It has been noted that EPS in a biofilm could immobilize metals prior to reaching the diffusive gel layer of a DGT.[118] Dunn *et al.* noted that substantial biofouling on a DGT suppressed copper accumulated by the device.[50] A wide variety of metals have been found to be immobilized by binding with EPS, and environmental pH influences which metals are bound.[119] Some metals may also be reduced to insoluble phases during this binding process.[120] As such, biofilm development may directly affect the measurements by DGT devices, preventing metals from reaching the binding layer and leading to underestimation of bulk solution concentration.

Many of the previously discussed methods of mitigation of fouling cannot be applied to DGT, which would require methods that are chemically inert and do not modify the diffusive boundary layer of the device surface. Some methods have been attempted; for example, for phosphate measurements, pre-treatment of polyethersulphone membranes with silver iodide effectively reduced biofilm formation but interfered with phosphate uptake.[121] Additionally, as the most effective chemical antifouling methods are metal-based, it is difficult to apply such methods to DGTs for labile metal measurement. In a study by Uher *et al.*, changing the membrane filter of the device to a polycarbonate membrane led to different biofouling communities developing, and quantification of metals differed between devices.[122] These findings may ultimately vary depending on the biodiversity of the fouling environment. Even in locations that are close geographically, as observed by Webster & Negri, different fouling organisms can dominate a biofilm and lead to different localised physico-chemical environments on the surface.[123]

This chapter aims to investigate biofouling in Atlantic and Mediterranean coastal and estuarine regions in the context of DGT devices. The study focused on the extent of fouling and speciation of fouling organisms in the early spring and late summer months on the polyethersulphone (PES) membranes of commercially available DGT devices. Correlation between the incidence of biofouling and factors such as trace metals in solution and temperature were considered. Longer deployments of PES membranes were performed to investigate the nature of potential biofouling species in varying geographical locations. This data was used to determine geographic and temporal distributions of fouling diatoms common in environmental monitoring deployments.

2.2 Methods

2.2.1 Sampling

DGT Device Membrane Deployments for Biofouling Analysis

DGT devices for biofouling analysis were deployed in conjunction with a trace metal monitoring program in 31 Atlantic and Mediterranean estuary and coastal sites. Figure 2.4. documents the deployment locations. DGTs were deployed during two

seasons: the wet season (between January and March) and the dry season (between August and October) in 2018. Devices were deployed between 1 − 1.5 m below the water surface for up to 7 days (t = 168 h), with most samples being collected after approximately 4 days (t = 96 h) of immersion. During the wet season, most sites had 1 DGT deployed for biofouling analysis, while most sites in the dry season had duplicate deployments. Following collection, the exposure window of the DGT was rinsed with deionised water and the device was placed in a plastic bag and stored under refrigerated conditions. In the laboratory, the device was opened, and the PES membrane filter was isolated. Samples were stored at 4 °C in a sealed container prior to analysis.
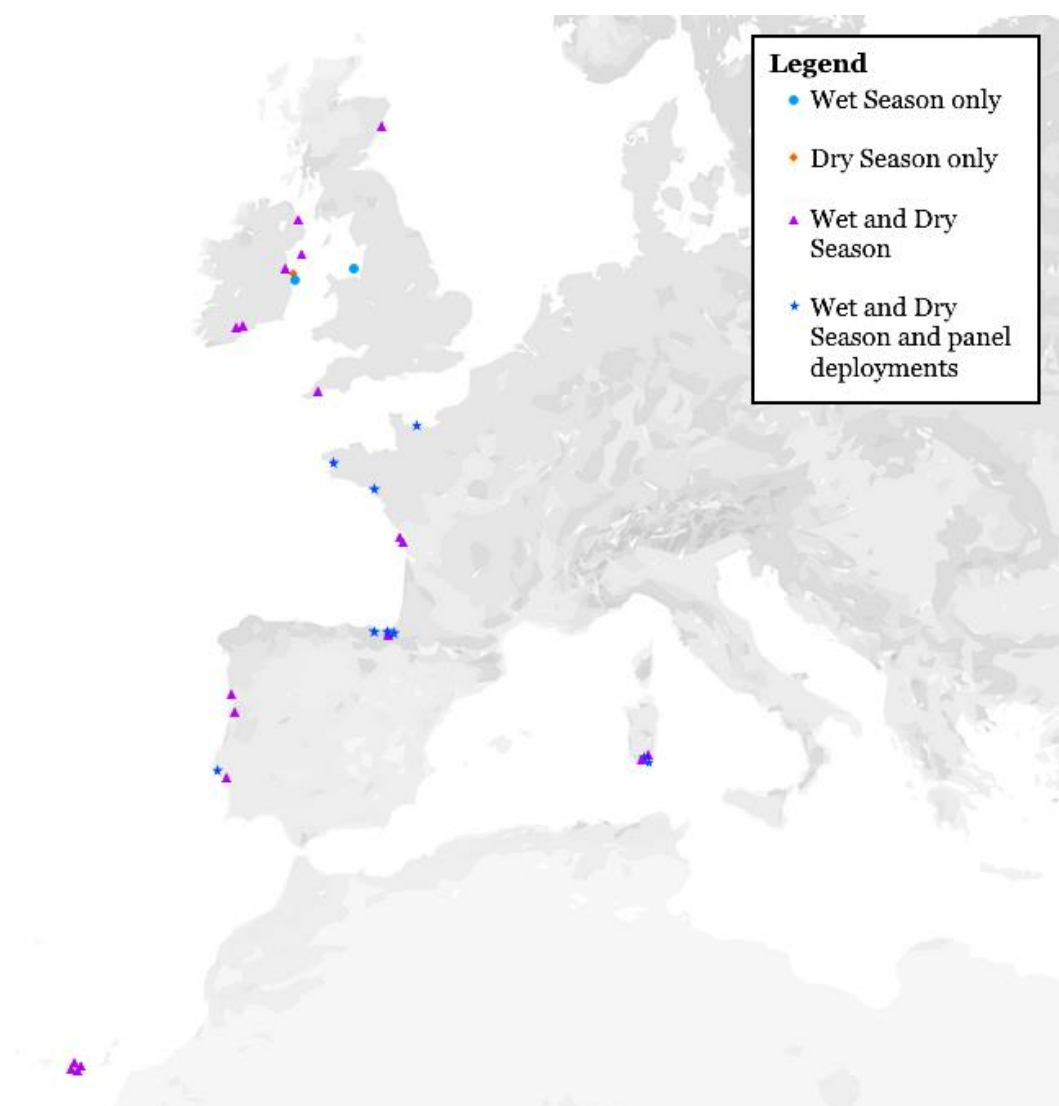
Figure 2.4. Atlantic and Mediterranean coastal and estuarine sites sampled under this study, divided by season. Fouling substrate panel deployments, which took place in the dry season, are marked.

Design and Deployment of Substrate Mounting Panels for Biofouling Analysis

Mounting panels for longer-term substrate biofouling analysis were prepared using 2 mm and 3 mm virgin polymethyl methacrylate (PMMA) fastened with uncoloured nylon screws and nuts. The plastics were washed with 1% v/v nitric acid to prevent metal contamination of simultaneous DGT deployments. Exposure windows were cut in the 2 mm thick PMMA panel using a laser cutter. The exposure window diameter, 2 cm, was equal to that of a standard DGT device.

PES membranes (Millipore Express®, 0.22 µm pore size) were deployed in duplicate within the substrate mounting panels. To prevent dislodgement during deployment, the membranes were affixed with a waterproof adhesive. The mountings were deployed for 14 days at 10 sites (marked with a star on the map in Figure 2.4) during the dry season sampling campaign (August to October 2018). Following collection, the surfaces of the mounting panels and the exposure substrates were rinsed with deionised water. A cover sheet of PMMA was attached to protect the membranes during transport, and the mounting panel was placed in a plastic bag and stored under refrigerated conditions. In the laboratory, the mounting panel was disassembled, the substrates were removed from the adhesive, and stored in sealed containers at 4 °C.

2.2.2 Analysis

Light Microscopy Protocol

Full images of the surface of the DGT membrane or the exposed section of mounted substrates were captured using a Keyence VHX2000E 3D digital microscope. Images were captured at 150 x magnification and the multiple image capture function of the microscope was used to generate a full surface scan. Where full scans were not possible (for example, in the case of heavily damaged membranes), scans of a subsection of the membrane were performed. Wet season DGT membranes were sectioned for other exploratory analysis and regions of approximately one-quarter of the device surface were scanned to estimate total cover. Features of interest noted on the surface were captured individually, and in the case of larger 3D features, the depth composition function of the 3D microscope was used to capture clear images of the features. Images were taken at 1 µm vertical intervals for depth composition.

Percentage Cover Analysis Protocol

To estimate the reduction in effective surface area of the device by the end of the deployment, a visual fouling percentage cover protocol was applied. ImageJ (imagej.nih.gov/ij/) image processing software was used to manipulate images. The exposed regions of full or subsection scans captured under the Light Microscopy Protocol had contrast increased, were inverted, and were converted to 8-bit black and white images. Using the Threshold function of ImageJ, the image was adjusted to a binary image, only including strong fouling features (captured in white), separating them from the substrate background (in black). The process of this image development is exhibited in Figure 2.5. Due to this contrast-based image processing, some weaker features of fouling, as well as reflective particles (such as sand or lone diatoms which have not secreted EPS) were not clearly resolved from the background, and as such the reported percentage covers would be slightly underestimated. Using ImageJ's Analyse function, the percentages of the image populated by white and black are calculated to determine overall visual percentage cover.
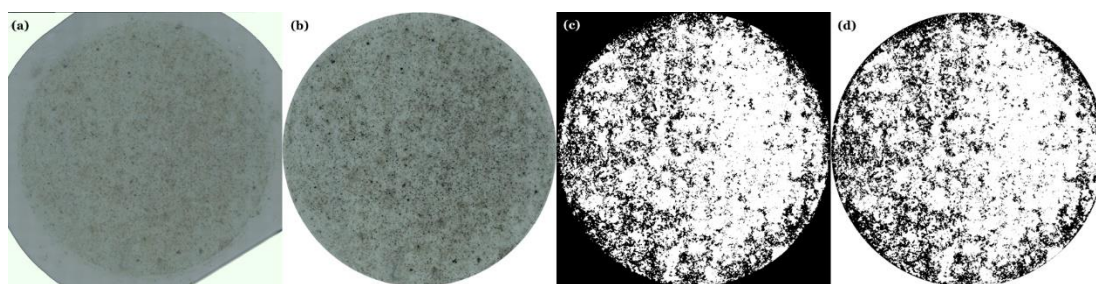
Figure 2.5. Determination of percentage cover for fouled membranes using the ImageJ image processing software from a full membrane scan (a) to a binary representation of fouling features in the exposure window (d).

Scanning Electron Microscopy Sample Preparation and Analysis

Samples were dried at 30 °C overnight to remove excess water from the membranes before preparation for Scanning Electron Microscopy (SEM) analysis. Once dried, the membranes were transected and cut into quarters, providing both edge and central fouling of the exposure window. The membrane subsections were mounted on a 26 mm carbon tab (Agar Scientific), and the samples were gold coated using a supper coater (Agar Scientific). Samples were coated for 30 seconds at a sputtering current of 30 mA and argon pressure 0.08 bar, approximately 40 mm from the target. Samples were analysed using the Hitachi S-3400 SEM. Fouling features of note and overview images of the membrane surface were captured.

Diatom Identification Protocol

Diatoms and other fouling species were captured under SEM in accordance with the Scanning Electron Microscopy Analysis protocol. Identification was performed of whole diatoms and fragments, where possible, visually with the aid of reference documentation including Round *et al.*'s *The Diatoms: Biology and Morphology of the Genera*, the Academy of Natural Sciences Philadelphia *Diatom New Taxon File*, and the National University of Ireland Galway *AlgaeBase*.[103,124,125]

Trace Metal and Temperature Analysis for Correlation Studies

Simultaneous sampling of water for trace metal analysis was performed during the short-term wet and dry season at the depth of deployment. Samples were analysed externally for trace metal content via Inductively Coupled Plasma Mass Spectrometry (ICP-MS) and stripping voltammetry (SV). All ICP-MS trace analysis and a majority of the SV trace analysis were performed by other researchers. Temperature was taken at regular intervals during deployments and the overall average temperature was obtained. These results were compared to percentage cover of fouling on the PES membrane surfaces to investigate correlation with these external factors.

2.3 Results

2.3.1 Fouling Cover

The visual fouling coverage percentage of the exposed PES membranes is documented in Table 2.1. Due to the density of the data, this table omits samples deemed to be minimally fouled (<1% total surface coverage). 14 wet season samples and 19 dry season samples are omitted under this stipulation. The Deba River in the Basque Region, northern Spain, exhibited the highest fouling percentage cover in the wet season sampling (37.31%) and the 14-day dry season deployments (99.74%). In the dry season, the Molo Rinascita site at Cagliari, Sardinia, exhibited the highest fouling percentage cover (54.06%).

Table 2.1. Fouling percentage covers for sites in both wet and dry seasons, with fouling levels greater than 1% total surface coverage.

Region	Site	Site Type	Season	Days Deployed	Percentage Cover
Basque Region	Deba	Estuary	Wet	4	37.3
			Dry	4	2.1
			Dry	14	99.7
	Lezo	Estuary	Wet	4	1.8
			Dry	14	39.6
	Museo	Estuary	Dry	14	11.8
England	38A Irish Sea	Coastal	Dry	3	2.7
	Belfast	Estuary	Wet	7	3.1
	Fal	Estuary	Wet	3	3.4
			Wet	4	3.3
Ireland	Alexandra Basin	Estuary	Wet	4	1.7
			Dry	2	1.1
			Dry	4	1.1
	Dublin Bay 4	Coastal	Wet	15	3.1
	Cork M69	Estuary	Wet	4	21.7
	Cork M70	Estuary	Wet	4	1.8
			Dry	4	1
France	Port En Bessin	Coastal	Wet	5	2.5
			Dry	4	6.5
			Dry	14	18.9
	St Nazaire	Coastal	Wet	3	1.9
			Wet	4	11.2
			Dry	2	5
			Dry	4	15.1
			Dry	14	18.3
	Terenez	Coastal	Dry	4	2.1
	Fontenelle	Estuary	Wet	5	4.3
	Saumonard	Coastal	Wet	5	9.9
Portugal	Aviero	Estuary	Wet	4	1.5
			Dry	2	2.2
			Dry	4	1.6
	Porto	Coastal	Wet	5	1
			Dry	4	5.2
	Tagus	Coastal	Wet	4	13.8
			Dry	2	38.3
			Dry	4	25.1
			Dry	14	37.9
	Sesimbra	Coastal	Wet	4	1.4
Gran Canaria	Taliarte	Coastal	Wet	7	3.8
			Dry	4	1.3
	La Luz	Coastal	Wet	7	1.2
Cagliari, Sardinia	Molo Dogana	Coastal	Wet	4	1.5
			Dry	4	8.9
	Molo Ichnusa	Coastal	Dry	4	5.7
	Molo Rinascita	Coastal	Dry	4	54.1
			Dry	14	17.1
	Sant Elmo	Coastal	Dry	4	5.9
			Dry	14	59.4

2.3.2 Impact of Seasonality, Temperature and Trace Metal Concentration on Early Biofouling

To determine seasonal impact, significance of difference of means between wet and dry season fouling percentage coverage was examined by performing a two-sample t-test. This test showed no significant difference ($p > 0.05$) between mean fouling in each season. However, it is important to note that the surface areas considered in each season differ, as the wet season samples were subsectioned prior to analysis and therefore is an estimate of total percentage cover.

Temperature and trace metal concentrations were compared to biofouling percentage cover across a number of matrices (total data, site type, season, and site type per season). Across these matrices, temperature showed no correlation with total biofouling coverage, with the strongest correlation noted when all wet and dry season estuarine sites were considered ($R^2 = 0.23$). Metals measured by ICP and SV, similarly, exhibited no correlation in many cases. Co measured by ICP ($R^2 = 0.38$) and Ni measured by SV ($R^2 = 0.82$) at dry season estuarine sites were the strongest correlations in this case.

2.3.3 Diatom Speciation at Studied Sites

Across the sites studied during the two seasons, 28 distinct genera of potential fouling diatoms of PES surfaces were successfully identified. For this count, only whole diatoms were considered potential fouling organisms. Fragments of other species, such as the distinctive valve structures of the *Hemidiscus* genera, were identifiable at multiple sites. However, these fragments may have originated from resuspended sediment and therefore would not represent active fouling species. Planktonic genera of diatoms were found to cause fouling predominantly on the deployed membranes, but some epilithic and benthic genera were also identified. Representative species in each genus are included in Table 2.2.

In total, 15 sites exhibited at least one identifiable diatom genera during at least one of the two seasons. The distribution of diatoms is represented in Table 2.3 grouped by the region of origin of the sample.

Table 2.2. Images of representative species of diatom genera identified in this study.
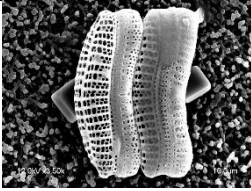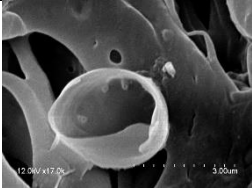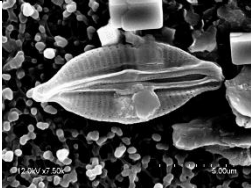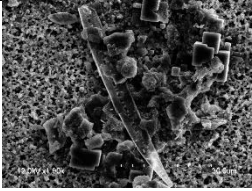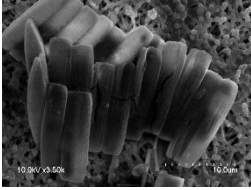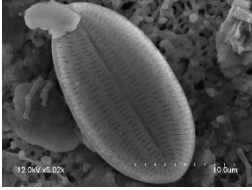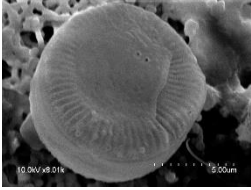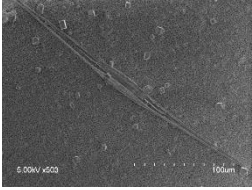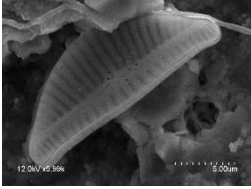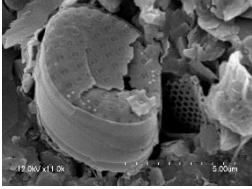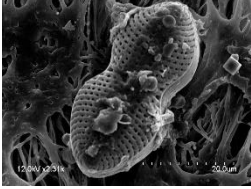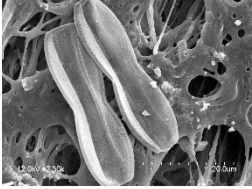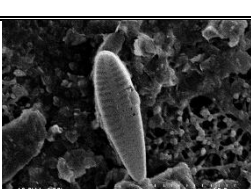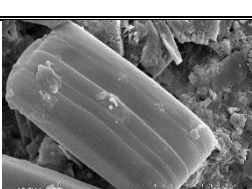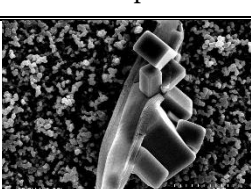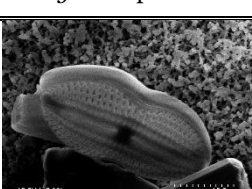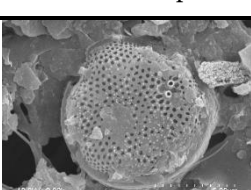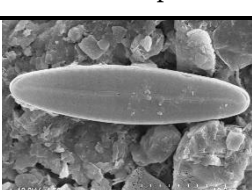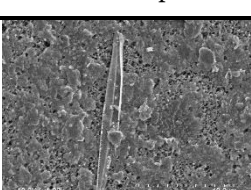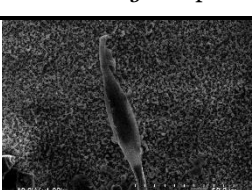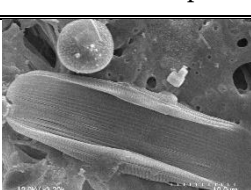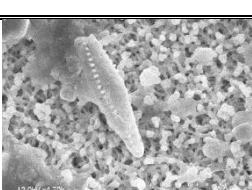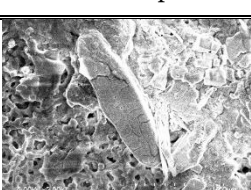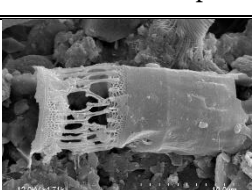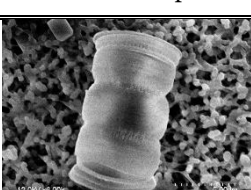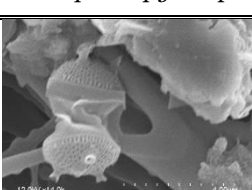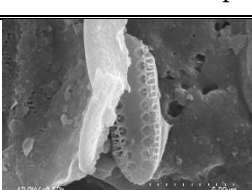
1: *Achnanthes* sp.	2: *Actinocyclus* sp.	3: *Amphora* sp.	4: *Bacillaria* sp.

5: *Catenula* sp.	6: *Cocconeis* sp.	7: *Cyclotella* sp.	8: *Cylindrotheca* sp.

9: *Cymbella* sp.	10: *Delphineis* sp.	11: *Diploneis* sp.	12: *Entomoneis* sp.

13: *Gomphonemopsis* sp.	14: *Grammatophora* sp.	15: *Halsea* sp.	16: *Lyrella* sp.

17: *Minidiscus* sp.	18: *Navicula* sp.	19: *Nitzschia* sp.	20: *Pleurosigma* sp.

21: *Proschkinia* sp.	22: *Pseudostaurosira* sp.	23: *Reimeria* sp.	24: *Skeletonema* sp.

25: *Staurosira* sp.	26: *Stephanopyxis* sp.	27: *Thalassiosira* sp.	28: *Thalassionema* sp.

Table 2.3. Sites at which diatoms were observed under this study, and diversity at each site. The numeration corresponds to the observed species in Table 2.2.

Region	Site Name	Site Type	1	2	3	4	5	6	7	8	9	10	11	12	13	14	15	16	17	18	19	20	21	22	23	24	25	26	27	28
Basque Region	Deba	Estuary	*	*	*		*	*		*	*			*	*				*	*	*									
	Lezo	Estuary	*															*	*	*	*	*	*					*		
	Museo	Estuary	*		*			*		*				*			*	*	*	*	*	*	*							
United Kingdom	Belfast	Estuary																		*										
Ireland	M69	Estuary			*															*					*					
	Alexandra Basin	Estuary																	*	*										
	Dublin Bay2	Coastal										*						*											*	
Portugal	Aviero	Estuary	*		*			*						*					*	*	*	*	*							
	Tagus	Coastal												*			*	*	*							*	*		*	
France	Port En Bessin	Coastal			*		*	*						*		*	*		*	*				*		*				*
	Saint-Nazaire	Coastal			*			*	*					*					*	*	*					*			*	
Gran Canaria	La Luz	Coastal			*		*	*		*				*						*										
	Taliarte	Coastal						*								*						*								
Cagliari, Sardinia	Sant Elmo	Coastal	*	*	*		*	*					*	*	*					*	*	*				*			*	
	Molo Rinascita	Coastal		*					*									*											*	

48

2.4 Discussion

2.4.1 Biofouling Coverage of DGT Devices

As discussed previously, biofilm development on deployed DGT devices can directly affect the device's uptake of trace metals. In this study, visual fouling at many sites was minimal during both seasons when deployment periods were constrained to less than 5 days (less than 1% surface coverage in most cases). The most heavily fouled sample was the 14-day deployed PES membrane at the Deba River, which was almost entirely covered by fouling (99.74% total coverage) and a developed EPS layer is evident under SEM. As can be seen in Figure 2.6, the fouling includes a rich community of fouling diatoms, including almost total coverage by populations of the *Achnanthes* and *Amphora* genera.
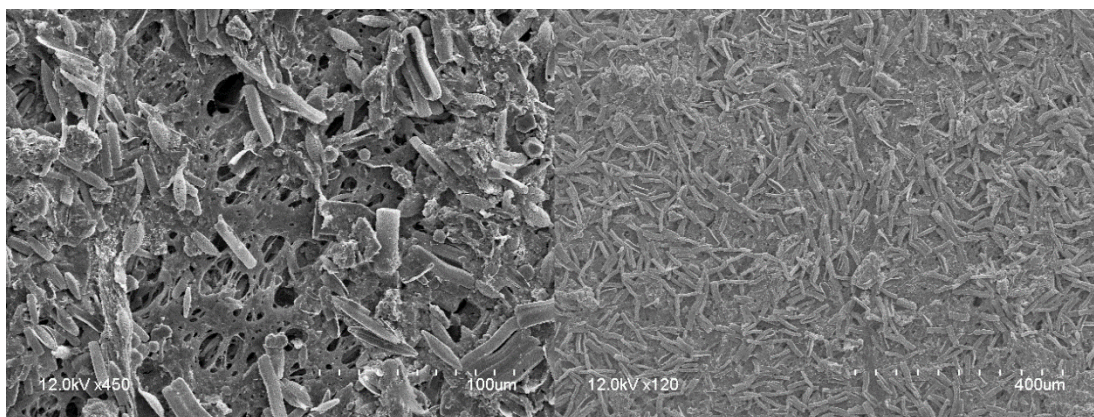
Figure 2.6. SEM imaging of the surface of the PES membrane deployed at the Deba River, Basque Region for 14 days. Dominance of the *Achnanthes* diatom genus can be seen, and many species of the *Amphora* genera are also visible.

Development of fouling on the surface of the membrane with respect to time in the dry season is represented in Figure 2.7. While there are heavily fouled outliers at some sites despite early collections (such as at Tagus River, Portugal on Day 2), the majority of the membrane are less than 1% fouled when deployments are limited to 4 days. Following 14-day deployment periods, surface fouling varied between 11% and 99.74% coverage. Suggestions have been made by many previous authors that DGT deployments are ultimately limited by the eventual impacts of biofouling. Recent work by Uher *et al.* suggests that limiting deployments to a period of 5-8 days would minimize biofouling impact while allowing equilibration of the device with the bulk solution, while providing a useful time-integrated assessment of environmental contaminants.[117] The present study supports this suggestion due to the low incident of fouling in both seasons for deployments lasting less than 7 days. However, certain

sites such as the Molo Rinascita site at Cagliari, Sardinia, exhibit heavy fouling within 4 days (54.06% total coverage). Despite the proximity of the four Cagliari dock sites sampled, no nearby site experienced similar levels of fouling, with 8.9% being the closest value. While this is an exceptional scenario within the current dataset, it highlights the challenge that biofouling may pose to even short-term DGT deployments in closely related sites.
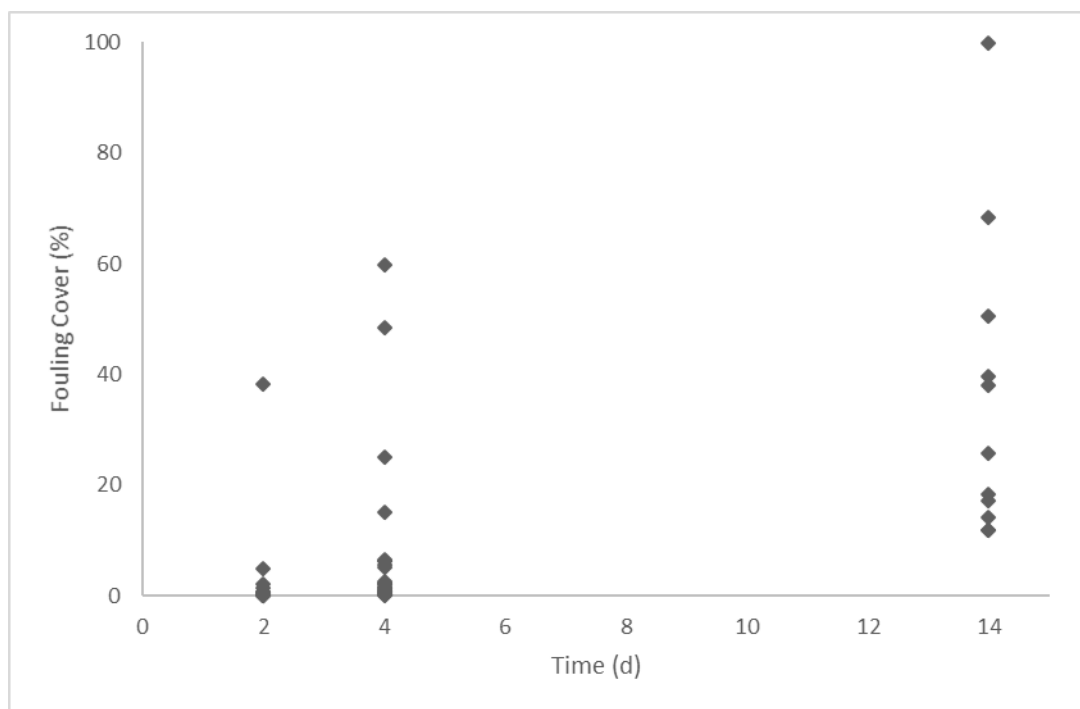
Figure 2.7. Fouling percentage coverage on deployed PES membranes following collection at various time intervals.

2.4.2 Impact of Seasonality, Temperature and Metal Concentration on Fouling Environments

At many sites, the impact of biofouling was directly influenced by the season in which the sampling occurred. Sites which experienced little fouling in the wet season, such as the Cagliari sites, exhibited increased fouling during the dry seasons. The higher temperatures in this season may have provided a more suitable environment for the growth and proliferation of certain fouling organisms. As fouling organisms such as diatoms have life spans of only a few days, the differing conditions of each season may be more hospitable to certain fouling organisms. Diatoms identified under this study are categorized by season of appearance at each site in Table 2.4. Some dry season samples, such as samples from the Sant Elmo site in Cagliari, exhibited macrofouling.

Table 2.4. Diatom fouling communities separated by season of organism observation.

Site Name	Season	1	2	3	4	5	6	7	8	9	10	11	12	13	14	15	16	17	18	19	20	21	22	23	24	25	26	27	28
Deba	Wet						*	*		*				*					*	*									
	Dry	*		*			*	*					*						*	*									
Lezo	Wet																		*										
	Dry	*															*	*	*	*	*	*					*		
Museo	Wet																		*	*									
	Dry	*		*					*				*			*			*			*							
Belfast	Wet																												
	Dry																		*										
M69	Wet			*															*					*					
	Dry																												
Dublin Bay 2	Wet																	*											
	Dry										*																	*	
Alexandra Basin	Wet																												
	Dry																	*	*										
Port En Bessin	Wet																												
	Dry			*			*						*		*	*	*	*	*	*					*				*
Saint-Nazaire	Wet			*			*	*					*			*		*	*				*		*			*	
	Dry			*			*						*					*	*	*									
Aviero	Wet	*		*			*										*	*	*	*	*	*							
	Dry				*		*										*	*	*							*			
Tagus	Wet												*					*	*										
	Dry																	*	*						*				
La Luz	Wet			*					*				*							*									
	Dry																												
Taliarte	Wet												*		*				*	*	*								
	Dry																												
Sant Elmo	Wet																								*				
	Dry	*	*	*		*						*		*			*		*	*	*				*			*	
Molo Rinascita	Wet							*									*												
	Dry	*	*	*																								*	

However, there was no statistically significant difference ($p > 0.05$) between wet and dry season fouling coverage, as some sites (such as the Lough Mahon transitional site in Cobh, Ireland) exhibited much greater fouling in the wet season. Similarly, regardless of site grouping there appeared to be little correlation between biofouling surface coverage and temperature. Water temperature has been cited as a critical factor in biofilm proliferation in a number of studies,[126,127] and the absence of correlation in this case suggests that the many variable parameters in this study give rise to wholly different fouling environments. The influence of temperature may not have been discernible following the short-term deployments which resulted in predominantly microalgal and bacterial fouling.

Stronger correlations were noted when the trace metal concentration of the surrounding waters were considered. Trace Ni measured by SV provided the strongest correlation with fouling coverage ($R^2 = 0.82$), followed by Co measured by ICP ($R^2 = 0.23$), when dry season estuarine sites were selected. While weaker, similar correlations are seen across a number of comparison matrices, and with Ni measured by ICP. The SV protocol, which will be discussed in more detail in Chapter 3, measures total Ni concentration following UV irradiation of filtered samples to break down organic matter. A study by Baeyens *et al.* suggests that labile Co, alongside other micronutrients, may be a limiting or co-limiting factor for the growth of diatoms.[91] Ni has been demonstrated to be required for the production of certain enzymes in diatoms, such as urease and Ni-containing superoxide dismutase, but high levels of this trace metal induce toxic effects and limit growth.[128,129] In the present study, trace Ni varied between 3-20 nM. Growth curves by Oliviera & Nantia suggest that within this range, there would be a proportional increase in growth before reaching stationary phase, supporting the current findings.[128] However, the availability of Ni is only one of many factors which may influence growth of these organisms, and the availability of other elements such as silicon, nitrogen and phosphate, which were not examined under this study, are each limiting to diatom growth.

2.4.3 Geographical and Seasonal Distribution of Fouling Diatoms

Geographical distributions of diatom genera present at three or more sites are displayed in Figure 2.8. Many diatom genera were identified in only one region: *Actinocyclus*, *Catenula* and *Diploneis* in Sardinia, *Delphineis* and *Reimeria* in Ireland, *Thalassionema* and *Pseudotaurosira* in France, *Cymbella* and

Stephanopyxis in the Basque Region, and *Bacillaria* and *Stuarosira* in Portugal. *Navicula* was the most commonly identified fouling genera, appearing in every region studied. *AlgaeBase* reports over 1,350 distinct species of *Navicula*, and it is generally accepted to be a ubiquitous planktonic genus in both fresh and marine waters.[125]

Certain genera were distributed across wide regions but absent from other studied sites. The *Cocconeis* and *Entomoneis* genera were present across the Atlantic coast from the Canary Islands to northern France at both coastal and transitional sites, but absent from the Irish Sea and Sardinian sites. *Minidiscus* occurred across a similar region but was present in the Irish Sea and absent from the Canary Islands sites. Select species were distributed across the Mediterranean, the Basque Region, France, and Portugal, including *Lyrella*, *Achnanthes*, *Skeletonema* and *Pleurosigma*. Certain genera were exclusively marine (*Cyclotella*, *Grammatophora*, *Skeletonema* and *Thalassiosira*), while the *Proschkinia* genera was only observed at estuarine sites.

Even when sites with similar physico-chemical parameters and low geographical resolution were considered, fouling environments differed considerably. Fouling on the samples deployed in the Deba and Oiartzun Rivers, the mouths of which are approximately 35 km apart, were dominated by the *Achnanthes* and *Entomoneis* fouling diatom genera respectively following 14-day deployments. While the *Amphora* genus was present at both sites, more diversity was noted at the Oiartzun River site Museo, where at least four distinct species were identified (Figure 2.9). Fouling at the M69 and M70 sites, representing the Lough Mahon and Ballynacorra transitional sites at Cobh, Co. Cork, Ireland, respectively (approximately 9 km apart), were similarly varied; while no diatom fouling was identified at the Ballynacorra site, the Lough Mahon site experienced wet season diatom and bacterial fouling. Most notably, the sites at Cagliari which were all within a semi-enclosed dock region (within 2 km of each other) experienced substantially different fouling environments, as can be seen when comparing the diatom communities of Sant Elmo and Molo Rinascita sites in Table 2.3.

Figure 2.8. Geographical distribution of diatom species present at three or more sampled sites across the Atlantic and Mediterranean regions.
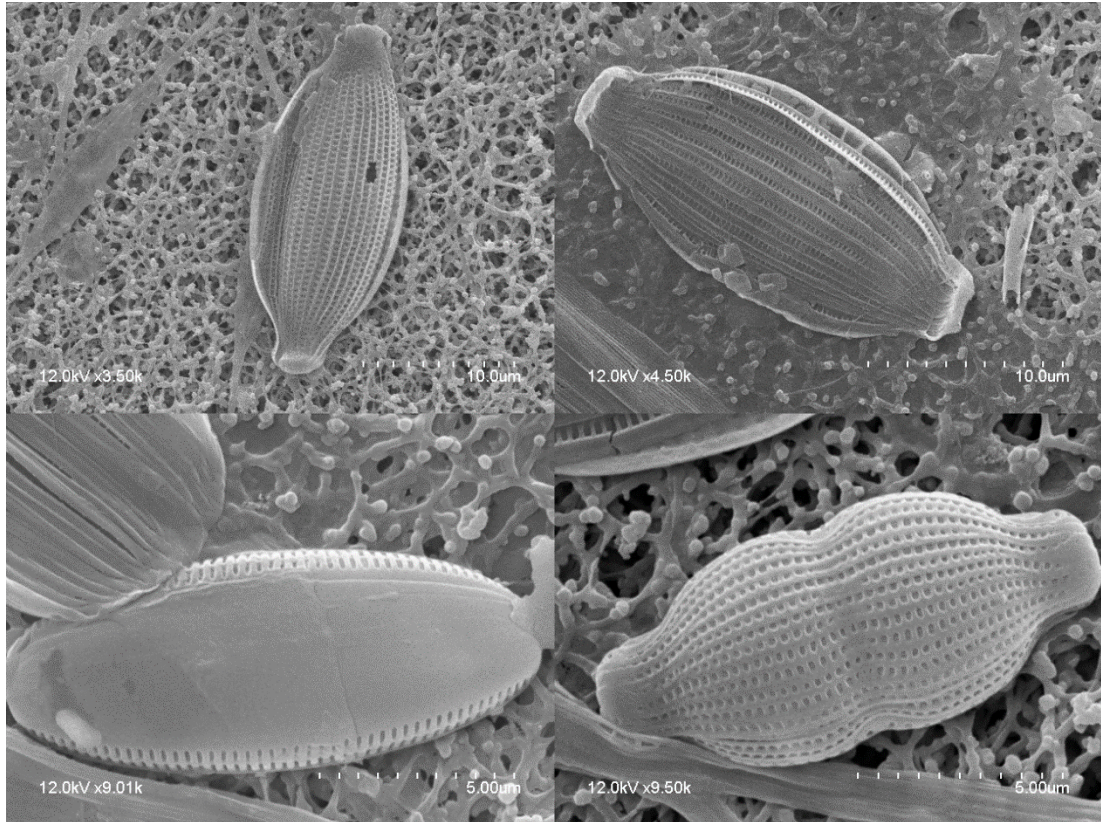
Figure 2.9. Variation of species of the *Amphora* diatom genus identified at the Oiartzun River, Basque Region.

Seasonal patterns in diatom communities can also be noted at certain sites. The *Achnanthes* genera appeared as a fouling diatom during the dry season only in the Basque Region, being absent during the cooler wet season. Similarly, the diatom fouling communities at the Sardinian sites (Sant Elmo & Molo Rinascita) and Port En Bessin in northern France were more diverse during the dry season, with only *Skeletonema* diatoms and bacterial fouling noted at these sites during the wet season. Conversely, certain sites, including the Lough Mahon transitional site in Ireland, Aviero in Portugal, and the Gran Canaria sites Taliarte & La Luz, experienced heightened fouling during the wet season with greater diatom diversity. At the Gran Canaria sites, this may partially have been due to the extended deployment times during the wet season, as documented in Table 2.1. However, as a general rule, diversity and dominance of fouling organisms increased during the dry season.

A limitation of the work as here presented is the identification of diatoms to genus level only. Wide geographical regions and a large diversity of fouling diatom genera were examined under this study, and this work presents a broad overview of the

diatom fouling environments at each site rather than detailed phytoplanktonic community assessments. The diversity of genera noted at each site is indicative of the unpredictability of the impact of biofouling on deployed surfaces, and the variation in fouling prevalence in closely related sites also highlights this. The previous recommendations made by Uher *et al.* suggesting that DGT deployments are optimally limited to 5-8 days are supported by this work,[117] with the majority of samples deployed for short periods being minimally fouled. However, further research into the development of biofouling on alternative membranes, and its overall impact on the trace metal accumulation of DGTs under controlled conditions, may offer a robust alternative allowing for longer-term deployments while minimising early fouling.

2.5 Conclusion

Biofilm development on the PES membranes commonly used as a membrane filter for DGT passive sampling devices was examined. The study found that at a majority of the studied sites, deployment of DGTs for 4 days or less resulted in minimal fouling covering (<1%). Deployment for up to 14 days resulted in biofilm coverages ranging from 11% to 99.74%. However, the impact of biofouling is an uncontrollable and unpredictable non-linear factor in such deployments; devices can often become heavily fouled after only a few days deployed, as has been observed in this study at a small number of sites. In addition, the season of the deployment was found not to significantly impact the percentage of fouling coverage on the device membranes, and this challenge can be encountered year-round. For the early diatom and bacterial fouling organisms, there was no correlation between temperature and biofilm formation after 4 days' deployment, and correlation was observed with few trace metals in solution, highlighting the unpredictability of early fouling.

Across the studied sites, 28 genera of the diatom phylum were identified as potential fouling organisms on the surface of the devices. Many of these genera were distributed across several regions in both coastal and estuarine sites, and in some cases exhibited almost total colonisation of the exposure window of the DGT device. The diversity of the observed genera, each with their own tolerance for environmental conditions, highlights the challenge of mitigating fouling on deployed surfaces in environmental waters, as some opportunistic fouling organisms will adhere to the surface regardless. The findings of this study support the deployment periods suggested by previous

authors of 5-8 days for standard DGT devices. However, there may be exceptions to this recommendation following enrichment events such as algal blooms, which may limit the deployment period of DGT for accurate quantitation of analytes. Investigation of other membrane filter compositions for biofilm resistance, and their impact on DGT trace metal accumulation under controlled conditions, is a worthwhile avenue of exploration to overcome this commonly highlighted limitation of DGT devices.

Chapter 3

Stripping Voltammetry for Trace Analysis of Priority Metals in Coastal and Transitional Waters

3.1 Introduction

Stripping voltammetry is a highly sensitive method of electrochemical analysis and has been successfully applied in the quantitation of a wide variety of analytes in many sample matrices.[130–132] Under ideal conditions, analyte concentrations to 10^{-10} M can be quantified accurately by stripping voltammetry methods, and simultaneous quantitation of several analytes can be performed using small volumes of sample.[131,133–135] The method is particularly advantageous for the analysis of trace metals in environmental waters, and can be applied to determine total metal concentration or the labile metal fraction, which may correlate with the bioavailable fraction of the metal.

Stripping voltammetry combines traditional voltammetric methods such as differential pulse voltammetry (DPV) or square wave voltammetry (SWV) with an analyte pre-concentration step on an electrode surface. Depending on the electrochemical properties of an analyte of interest, one of three pre-concentration methods are used. Anodic stripping voltammetry (ASV) and cathodic stripping voltammetry (CSV) deposit the analyte on the electrode by electrochemical means, whereas adsorptive stripping voltammetry (AdSV) involves non-electrochemical methods of adsorption to the working electrode in a separate step prior to analysis.[131]

Analytes of interest are firstly pre-concentrated at the surface of an electrode, and subsequently removed by a sweeping potential, inducing a change in current.[134] A stationary electrode such as a hanging mercury drop electrode (HMDE) or solid electrodes such as glassy carbon or gold, act as a point of aggregation for analytes of interest. An appropriate potential is chosen to allow for reduction or oxidation of the analyte, resulting in its deposition at the surface of the electrode or its incorporation into a mercury amalgam. During this deposition period, the solution is continuously stirred to ensure convection of analytes to the electrode surface.[130,133] A sweeping potential is subsequently applied across a specific range to strip the deposited analytes from the working electrode. The current induced by the stripping process results in a peak proportional to the analyte's concentration, allowing for quantitation of the analyte.[136] Each analyte has a characteristic potential at which it is stripped from the electrode, allowing for the simultaneous quantitation of several analytes under ideal operating conditions. A diagram of the stripping voltammetry process is presented in Figure 3.1.
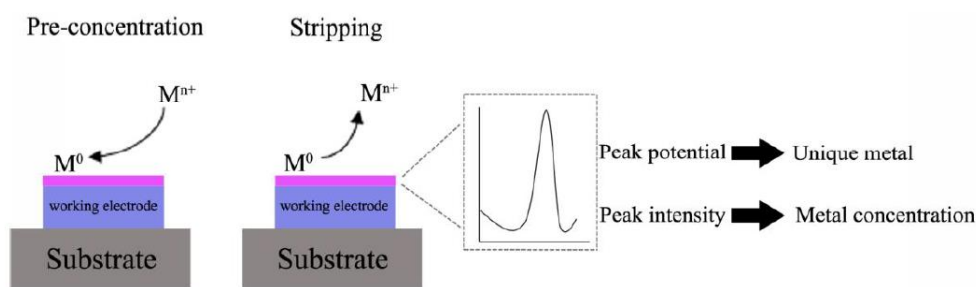
Figure 3.1. A representative diagram of the stripping voltammetry process for a metal species (M) reduced during pre-concentration. Reproduced from March *et al*.[136]

ASV and CSV are differentiated by the direction of the sweeping potential with respect of the initial electrodeposition potential. Under ASV, the potential is swept towards positive potentials to oxidise species that are reduced on the electrode during electrodeposition, whereas CSV applies a sweep towards negative potentials to reduce oxidised species.[134,137] Soluble cationic trace metals can typically be measured by ASV, with some exceptions, while CSV can be applied to metals as well as anionic species and organic compounds.[130] For species that are not electroactive, or will not be deposited on the electrode under certain conditions, AdSV must be conducted by complexation of the analyte prior to pre-concentration. A species that will adsorb to the electrode is formed, and the potential is subsequently swept towards either negative or positive potentials to strip the complexed analyte to induce a current.[133]

The sensitivity of stripping voltammetry allows for the quantitation of analytes at µg/L to ng/L concentrations,[135] and reduces sample manipulation by eliminating procedural steps such as pre-concentration and matrix suppression, overall reducing the risk of contamination. Sensitivity of the method is improved by choosing appropriate waveforms, with square-wave and differential pulse waveforms commonly applied; these waveforms combine cycling pulses and staircase waveforms and reduce background noise by suppressing capacitive currents.[134,138] In addition, when trace metals are analysed, information regarding speciation can be obtained by adjustment of operating procedures.[130,139] Free ions and complexed species can be differentiated by observing shifts in peak potential, which is not possible using conventional total metal analysis procedures such as AAS or ICP.[130]

When mercury-based electrodes are used, such as the HMDE or a solid electrode with a mercury film coating (mercury film electrode, MFE), ASV can be used to measure a range of over 20 metals. This is limited to metals that are readily reduced for incorporation into a mercury amalgam and oxidised to be released, in a reversible redox process.[138] Metals such as Ni cannot readily be measured on mercury electrodes and must first be complexed with a ligand such as dimethylglyoxime (DMG), which is highly selective for Ni and Co at pH 9.2.[137,138] Similarly, metals such as Al, V and Fe require complexation with the Solochrome Violet RS ligand prior to electrodeposition on mercury electrodes.[132,140] However, these methods which are highly selective for given metals interfere with colloidal or otherwise non-labile forms and hence can only be considered a quantitation of total metal concentration. Other electrode types are more suitable for certain analyses; for example, certain oxidizable species are detected optimally by platinum solid electrodes and wax-impregnated glassy carbon electrodes (GCE).[132]

Stripping voltammetry is advantageous over other metal analysis techniques in the analysis of environmental samples. The method is particularly suited to waters of a high ionic strength such as seawater, as the salts present are used as a supporting electrolyte without the addition of other chemicals.[138,141] High salt solutions are challenging to measure via ICP and AAS due to interferences caused by the matrix, making stripping voltammetry an optimal choice to minimize sampling handling.[130] The compact nature of voltammetric instrumentational also allows for it to be performed *in situ* aboard ships easily.[142] Studies have been conducted in waters of various ionic strengths, ranging from river water investigated for Cr speciation using cathodic AdSV by Bobrowski *et al.*,[139] to Ariel & Eisner's investigation of trace metals in Dead Sea brine by ASV.[141] Researchers such as Valenta *et al.* and Florence document in detail the sampling, handling, and analysis procedures of trace metals in seawater.[135,138]

However, the direct analysis of environmental waters by stripping voltammetry is impeded by the presence of dissolved organic matter (DOM). DOM is an unpredictable component of the sample matrix, consisting of various organic compounds such as polysaccharides, proteins, acids and oils, and can supress peaks and cause peak shifts towards cathodic potentials by electrochemical adsorption to the electrode surface.[49,130] This adsorption also reduces the availability of active sites

on the surface for electrodeposition of analytes and may impede the reversibility of redox reactions.[130] DOM can also directly complex with trace metals in solution, potentially forming non-electroactive organic compounds with metals such as Ni.[42,138] Brezonik *et al.* studied in detail the effects of DOM constituents separately on ASV signals, and noted peak suppression by gelatin and merging of the Cu peak with the background signal caused by surfactants.[49] As such, environmental samples, particularly high DOM samples originating from marshes or rivers receiving wastewater effluent, should therefore be UV irradiated to destroy organic material and resuspend the metal cations in solution.[49]

For the purposes of stripping voltammetry, liquid mercury-based electrodes such as the HMDE and the MFE are optimal, offering low detection limits, minimal background noise, and a wide window of operating potentials.[136] The HMDE is also self-cleaning, as it purges its mercury drop prior to electrodeposition and replaces it with another drop of a controlled surface area.[132] However, the environmental concerns regarding the use of liquid mercury, as well as the personal health hazards to analysts, highlights the necessity of the development of alternative solid and film-based electrodes. March *et al.* present a comprehensive study of the advances in the development of alternative electrodes.[136] Of particular interest is the bismuth film electrode (BFE) which can be plated on many solid electrodes similar to the MFE, and provides well-defined and reproducible responses.[143] Rather than forming an amalgam, BFEs form alloys with metals such as Pb and Cd and can increase separation of these metals over MFEs.[136] However, one of the critical limiting factors of BFE use is the limited potential range and poor chemical stability, as bismuth is more easily oxidised than mercury can is more readily stripped from the electrode surface.[136,143,144] BFEs also cannot be used to quantify Cu, due to oxidation of the film occurring at the stripping potential of Cu^{2+}.[144,145]

In recent years, graphene-based electrodes such as planar graphene electrodes and carbon nanotubes (CNT) have been investigated due to their mechanical strength, chemical stability, wide potential window, and excellent conductive properties.[144,146] CNT electrodes significantly improve Pb^{2+} detection over bare GCEs,[136] and the combination of graphene and bismuth film methods has been a promising development, with the simultaneous detection of Pb, Zn and Cd achieved using BFE-coated CNT electrodes by Hwang *et al*, with low detection limits for all but Zn.[145]

Lower detection limits for Zn were achieved by Lee *et al.* using an electrochemically plated graphene-bismuth mixed film.[146] As CNT production requires expensive instrumentation and toxic chemicals, this method presents a more environmentally friendly alternative. However, despite the environmental and health concerns, liquid mercury-based electrodes remain optimal for regular routine electrochemical analysis.

In this working chapter, the use of ASV and cathodic AdSV is adapted for the analysis of Ni, Cd, and Pb in coastal and transitional water sites of the Atlantic Ocean. HMDE and MFE electrodes were used to allow for optimal detection limits of these trace metals. Under the EU WFD (2000/60/EC), these metals are categorised as priority substances which must be managed to achieved GES for EU water bodies.[10] Cd and Pb in particular are contaminants of great ecological concern due to their persistence in organism tissues, and chronic toxicity can occur if contamination events are repeated. The adapted methods are then applied to field samples, and the concentrations of Cd, Pb and Ni determined by voltammetric analysis were compared to EU WFD guideline levels and other studies performed at the chosen sites simultaneously to investigate potential contamination events, and to validate the suitability of stripping voltammetry as an analytical tool.[11]

3.2 Methods

3.2.1 Sampling

Environmental waters for the determination of Cd, Pb, and Ni were obtained at coastal and estuarine locations of France, southwest England, and the Basque region of northern Spain, as displayed in Figure 3.2. Port En Bessin is a harbour in the Bay of Seine and contamination may be as a result of local anthropogenic input by the harbour town, as it is not on the watercourse of the Seine.[147] The Saumonard sampling site is located in the Marennes-Oléron Bay, the largest farming region of the Pacific oyster in Europe.[148] Saint-Nazaire is located at the mouth of the Loire River, the longest river in France, and the Loire drainage basin covers 20% of France's landmass. In the Basque region, the Oiartzun River's morphology and industrial inputs such as paper mill discharges have led to heightened contamination in the past and was previously classified as a highly pressured region.[4] Two sites (Lezo and Museo) are sampled along the Oiartzun watercourse. The Fal River estuary in southwest England

has historically been contaminated by trace metals due to mining operations in the region, and trace metals deposited in the littoral sediment are well studied.[149,150] Samples were collected between September and October 2018.

Figure 3.2. Map of sampling sites examined under this study in the Basque region of northern Spain, at three French coastal locations, and in southwest England.

Two 50 mL grab samples of water were taken at each site. Samples were taken at a depth of 1 – 1.5 m below the surface and stored in polypropylene DigiTUBEs (SCP Science, 50 mL). The samples were filtered into clean DigiTUBEs onsite using DigiFILTER systems (SCP Science, Teflon filters, 0.45-micron pore size). The filtrate was acidified to pH 2 with 35 μL ultrapure concentrated nitric acid (HNO$_3$, 69-70% v/v). 50 mL of Milli-Q deionised water (18.2 MΩ) was filtered and acidified on-site as a field blank following the same procedure. Samples were stored at 4 °C prior to analysis. Certified Reference Materials (CRMs) for nearshore and estuarine water,

CASS-6 and SLEW-3 (National Research Council, Canada) were used to validate methods of analysis for each of the metals weekly. Water deionised to a resistance of 18.2 MΩ was used as a method blank.

3.2.2 Instrumentation and Voltammetric Cell Setup

For Ni analysis, an Autolab Potentiostat system (Metrohm AG) was used to control a HMDE consisting of a Multi-Mode Electrode Pro and silanized mercury capillary (Metrohm AG). High purity mercury (99.6%, Merck) was used. The voltammetry cell was mounted on a 663 VA Stand (Metrohm AG) and included the HMDE, a 2 mm diameter carbon counter electrode (CCE), and an Ag/AgCl reference electrode using 3 M potassium chloride (KCl, Chem-Lab) as a bridge electrolyte. To stir the solution a polyethylene terephthalate (PET) stirrer was attached to the rotor system.

For Cd and Pb analysis, a glassy carbon working electrode with a 5 mm working diameter (Metrohm AG) was used in conjunction with an Autolab Potentiostat. The working electrode was attached to the rotor system of a 663 VA Stand and functioned as a stirrer. The voltammetry cell included this electrode, a CCE, and an Ag/AgCl reference electrode with 3 M KCl bridge electrolyte.

In both cases, analysis was carried out in clean disposable PET vessels to minimise contamination between samples. Samples were deoxygenated using high-purity nitrogen gas passed through a secondary vessel containing Milli-Q deionised water (18.2 MΩ). The KCl bridge electrolyte solution was changed daily. Voltammograms were recorded using General Purpose Electrochemical System (GPES) software, version 4.9.007 (Metrohm AG).

3.2.3 Reagents

A mixed Cd and Pb stock solution (1 mg/L) was prepared in 18.2 MΩ deionised water from 1000 mg/L Cd and Pb standard solutions (Sigma-Aldrich, TraceCERT®) and acidified to pH 2 with ultrapure HNO_3 (Sigma-Aldrich, 69% v/v). The stock solution was prepared weekly, with subsequent working solutions prepared daily from this stock in 18.2 MΩ deionised water and acidified as above. An electrode conditioning solution was prepared by dissolution of 1 M ammonium acetate (Sigma-Aldrich) in

0.5 M hydrochloric acid. A deposition solution for MFE formation was prepared using mercury (II) nitrate to a final mercury concentration of 0.12 mM in 18.2 MΩ deionised water and acidified to pH 2 with ultrapure HNO_3. An electrode cleaning solution was prepared by dilution of 200 µL of the conditioning solution, and 500 µL of 1 M ammonium thiocyanate (Sigma-Aldrich) in 20 mL of 18.2 MΩ deionised water.

A Ni stock solution (1 mg/L) was prepared from a 1000 mg/L Ni standard solution (Fluka Analytical, TraceCERT®) in 18.2 MΩ deionised water and acidified to pH 2 as above. Stock and working solutions were prepared regularly as described above. A 0.05 DMG ligand (Sigma-Aldrich) solution was prepared to 100 mL using 18.2 MΩ deionised water and 1 mL of 30% w/v sodium hydroxide (NaOH). A 2 M ammonium chloride (Sigma-Aldrich) solution was used as a buffer. To adjust the pH of the solution to an appropriate working range for DMG complexation with Ni, 30% w/v NaOH was used.

3.2.4 Cadmium and Lead Analysis

Methods for the analysis of Cd and Pb by ASV were adapted from de Carvalho *et al.*[151] From the above method, the deposition duration of the MFE and the trace Cd and Pb in solution were extended to optimise analysis of lower concentrations. The GCE was prepared as follows: MicroPolish Alumina II (Buehler) was applied to a MicroCloth cleaning pad (Buehler) and the electrode working surface was polished by circular scrubbing on the cleaning pad for approximately one minute. Excess polish was removed from the electrode carefully using dust-free paper, avoiding excessive abrasion of the electrode working surface. The electrode was then sonicated for one minute in 18.2 MΩ deionised water, taking care to ensure the electrode did not contact another surface during sonication to prevent damage.

Following cleaning, the GCE was attached to the rotor and the system was cleaned with 1% HNO_3 and 18.2 MΩ deionised water, and then dried. Table 3.1 documents the operating parameters of the scans for MFE development: in normal cyclic voltammetry (CV) mode, a 50-cycle scan was performed using the prepared conditioning solution. The system was then cleaned as before, and in SWV analysis mode, a run was performed using the deposition solution. Mercury cations were

deposited on the working surface of the electrode in this step and the MFE was prepared for analysis.

Table 3.1. Table of operating conditions used for each procedure in the analysis of Cd, Pb and Ni, and the development of mercury film for Cd and Pb analysis by ASV.

Method	Ni Analysis	Cd/Pb Analysis	Cd/Pb MFE Conditioning	Cd/Pb MFE Deposition
Solutions	10 mL sample	10 mL sample	1 M ammonium acetate & 0.5 M hydrochloric acid	0.12 mM mercury (II) nitrate solution (pH 2)
	100 μL 0.05 M DMG	50 μL 69% nitric acid		
	100 μL 2 M ammonium chloride			
Purge Time (s)	500	500	0	400
Deposition Potential (V)	-0.8	-0.9	---	-1.3
Deposition Duration (s)	60	300	---	420
Equilibration Time (s)	10	10	---	10
Initial Potential (V)	-0.8	-0.9	-0.8	-1.3
End Potential (V)	-1.1	-0.3	0.8	-0.15
Step Potential (V)	0.00495	0.00495	0.1	0.00495
Mode	Square-Wave	Square-Wave	Cyclic Voltammetry	Square-Wave
Cycles	---	---	50	---

10 mL of a sample was added to a clean disposable PET vessel, and 50 μL of 69% v/v ultrapure HNO_3 was added to adjust the sample pH to an appropriate working range. The sample vessel was deoxygenated using 0.5 bar nitrogen gas. The operating conditions for sample analysis are documented in Table 3.1. Scans of this sample were performed in duplicate. Standard additions were then performed by the addition of 50 μL of an appropriate Cd and Pb working solution to the sample vessel, limiting exposure to air. In most cases, a 12 μg/L Cd and Pb working solution was suitable. The scans were run in duplicate as above, reducing the purge time to 120 seconds for the initial scan following addition. The standard addition protocol was performed in triplicate on each sample, to a total addition volume of 150 μL. An example voltammogram generated using this method using the SLEW-3 CRM is included in Figure 3.3. The system was rinsed with 1% HNO_3 followed by 18.2 MΩ deionised water between samples. The GCE was cleaned and mercury ions stripped by performing a 7-cycle scan in normal CV mode using the cleaning solution.
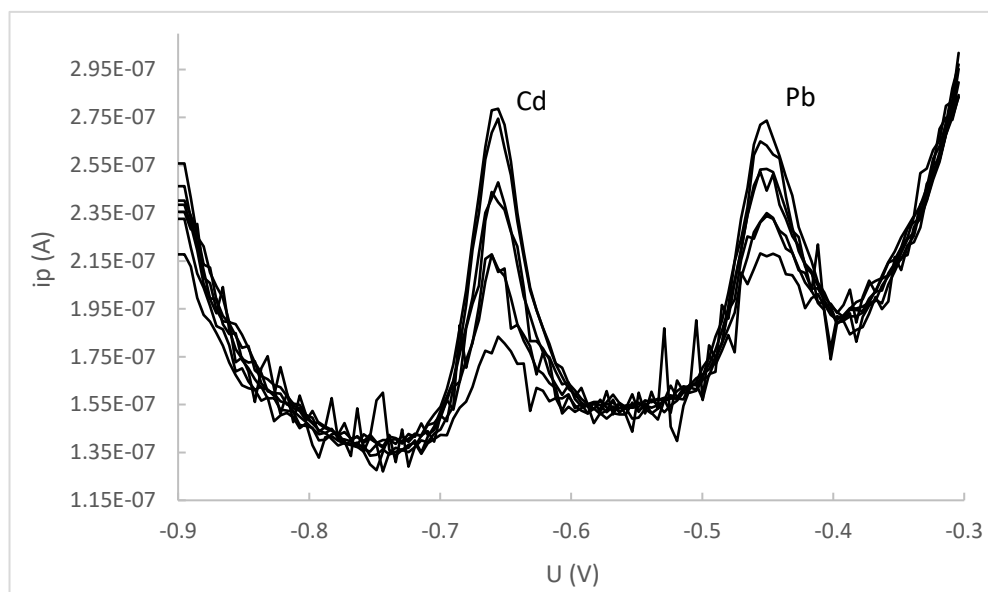
Figure 3.3. An example of combined voltammograms of Cd and Pb determined by ASV using an MFE, following standard addition procedures of a Cd and Pb solution to the SLEW-3 CRM. Using the operating procedures in Table 3.1, potential (U) was swept to induce changes in current (ip).

3.2.5 Nickel Analysis

Methods for the analysis of Ni were adapted from Cobelo-García *et al.* and Xue *et al.*[152,153] From these methods, the main alterations were the change of initial deposition potential. It was observed by Cobelo-García *et al.* that Ni stripping current increased at potentials more negative than -0.3 V, but the experiment was limited by the simultaneous quantitation of vanadium.[152] Xue *et al.* used a deposition potential of -0.6 V, and here the more negative -0.8 V potential is used.[153] The deposition duration was also adapted from these procedures and ultimately reduced to 60 seconds.

Prior to analysis, samples were transferred to boiling tubes and capped. A low-pour mercury lamp was used to irradiate the samples with UV light for one hour to break down organic matter. Samples were left to cool to room temperature (approximately 20 °C) following this procedure. Upon cooling, 10 mL of irradiated sample was added to a clean disposable PET vessel. 100 μL of 0.05 M DMG solution and 100 μL of 2 M ammonium chloride buffer was added to the sample. The pH was adjusted with 30% w/v NaOH as necessary, until the sample reached a DMG-Ni complexation pH range

of 8.7-9.5. The system was cleaned before and after runs. Nitrogen gas at 1 bar pressure was used to deoxygenate the sample prior to analysis. The operating conditions for sample analysis are documented in Table 3.1. The hanging mercury drop used in this experiment was 1 mm in diameter. Scans were performed in duplicate.

Standard additions to the sample were performed using a working solution of an appropriate Ni concentration. The concentration of these solutions ranged from 8 μg/L (typical for method blanks of 18.2 MΩ deionised water) to 200 μg/L (for the SLEW-3 CRM). 50 μL of the working solution was added and the scans were run as above, reducing the purge time to 120 seconds for the initial scan following addition. This standard addition protocol was performed in triplicate, to a total added volume of 150 μL. An example of this standard addition procedure being performed using the CASS-6 CRM is included in Figure 3.4.
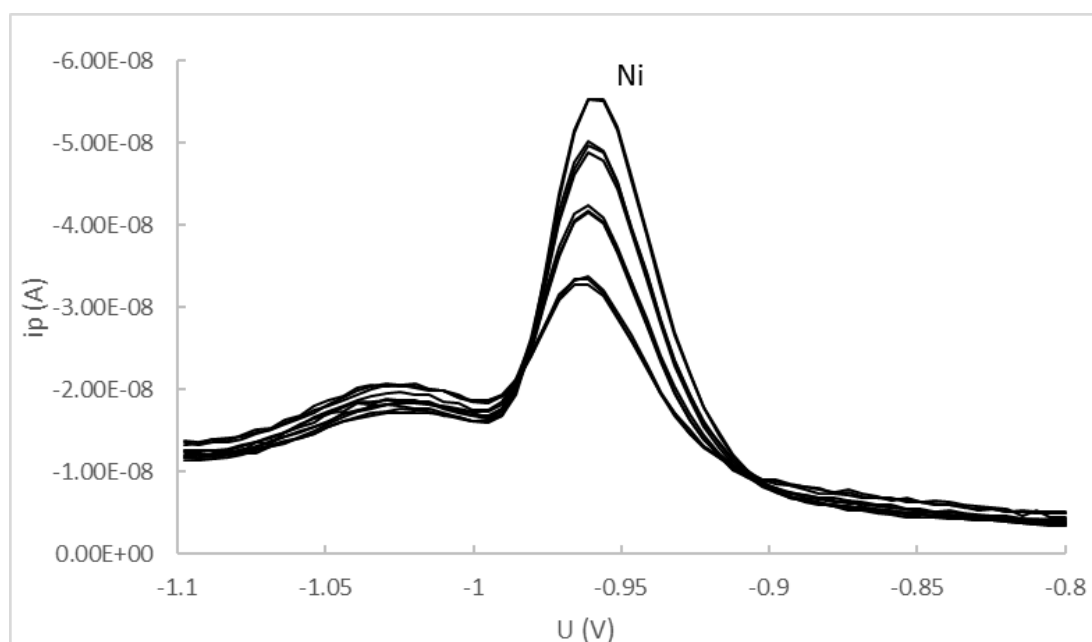
Figure 3.4. An example of combined voltammograms of DMG-complexed Ni determined by cathodic AdSV using a HMDE, following standard addition procedures of a Ni stock solution to the CASS-6 CRM. Using the operating procedures in Table 3.1, potential (U) was swept to induce changes in current (ip).

3.2.6 Comparison of ICP and voltammetric Ni concentrations

As the concentrations of Ni measured by cathodic AdSV should theoretically correlate with the total dissolved fraction, total metal analysis methods such as ICP should correlate with voltammetric concentrations. ICP samples were collected in tandem with the voltammetric samples, frozen at -20 °C, and subsequently filtered through a 0.45μm pore size filter and analysed by an external laboratory. Following analysis via ICP-MS, results were compared to voltammetric Ni.

3.3 Results

Standard addition plots were generated by determining the average current peak heights using either the automated peak search function of GPES, or the manual peak search function for peaks that were not accurately integrated using the automated function. Stripping potentials of Cd and Pb were approximately -0.65 and -0.45 V respectively, and stripping potential of Ni was approximately -0.98V following DMG complexation. Absolute values of the average peak heights were taken and graphed against the concentration of standard addition solution added. An example of such a graph, generated for Cd from a Fal Estuary sample, is shown in Figure 3.3.
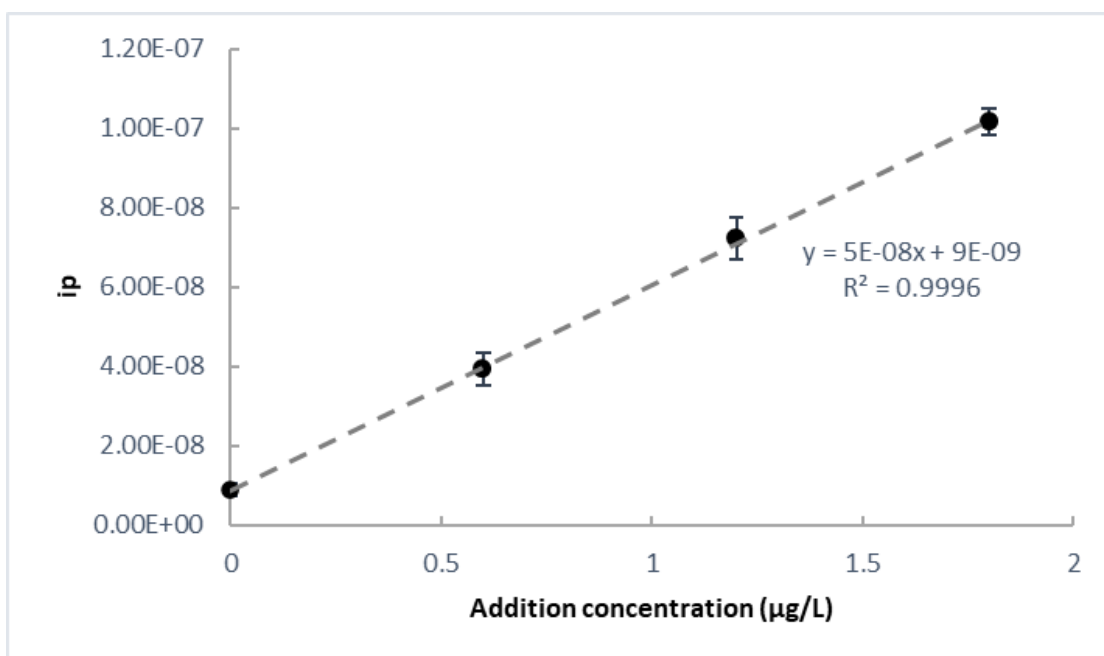
Figure 3.5. Standard addition plot (n=2) of Cd standard solution to a sample from Fal River Estuary, Southern England. Samples generated using the Cd/Pb ASV analysis method documented in Table 3.1 using an MFE coated on a GCE under square-wave waveform, deposition time 300 seconds at -0.9 V.

From each generated graph, the original concentration of the sample, C_o (µg/L) was determined using Equation 1. The y-intercept (c) was divided by the slope (m) and multiplied by the concentration of the added solution (C_a, µg/L). C_o was then determined by division by the initial volume, v_i (the volume prior to standard addition, in mL; 10.2 for Ni, 10.05 for Cd and Pb). Confidence intervals were also generated following procedures included in the Appendix. Significance testing between sites was performed using single factor ANOVA testing using a 95% confidence interval. Suspected outliers were tested using Grubbs' Test.

$$C_o = \frac{\left(\frac{c}{m}\right)(C_a)}{v_i} \qquad (1)$$

The CASS-6 and SLEW-3 CRMs were used to validate the method weekly, and the results of an example validation set are included in Table 3.2. In this set, recoveries for Ni and Cd ranged between 52.44 – 101.8% and 62.97 – 124.62% CRM concentration, respectively, while due to the impacts of background noise at low concentrations, Pb recoveries were highly varied (ranging between 27.86 – 816%).

Table 3.2. An example set of Certified Reference Material recoveries by ASV (Cd/Pb) and cathodic AdSV (Ni), performed weekly to validate methods.

	CASS-6			SLEW-3		
	Cd	Ni	Pb	Cd	Ni	Pb
Certified	0.0217 ± 0.0018	0.410 ± 0.04	0.0106 ± 0.004	0.048 ± 0.004	1.23 ± 0.07	0.009 ± 0.004
Detected	0.0198 ± 0.005	0.26 ± 0.024	0.034 ± 0.0199	0.036 ± 0.001	1.13 ± 0.051	0.018 ± 0.011
Recovery	62.97 - 124.62 %	52.44 - 76.76 %	27.86 - 816 %	67.31 - 84.09 %	83 - 101.8 %	53.85 - 580%

3.3.1 Results of Environmental Sample Analysis

Concentrations of Cd and Pb at the Oiartzun River, northern Spain

Table 3.3 documents concentrations of Cd and Pb found in samples from the estuarine sites of the Oiartzun River in the Basque region, northern Spain. Low concentrations of Cd were detected at both sites, with concentrations generally below the LOD (<0.009 µg/L) at the coastal town of Pasaia, where the Museo site is located. Further upstream, Cd concentrations at the town of Lezo were heightened, with one sample (Lezo Day 1 Low Tide Replicate 1) exceeding 0.1 µg/L. In contrast, Pb concentrations at the Museo site were significantly ($p < 0.05$) and consistently higher than at Lezo

across the sampling period, and there was a 20-fold difference between concentrations observed at low tide on Day 3.

Table 3.3. Cd and Pb concentrations measured by ASV (documented in Table 3.1) at the two selected Oiartzun River sites in the Basque region, northern Spain.

Site Name	Type	Day	State of Tide	Cd concentration (µg/L)	Pb concentration (µg/L)
Museo	*Estuary*	1	Low	<LD	2.9 ± 0.1
				<LD	2.5 ± 0.3
			High	<LD	2.8 ± 0.3
				0.042 ± 0.026	4.3 ± 0.4
		3	Low	<LD	3.3 ± 0.3
				<LD	3.1 ± 0.3
			High	0.060 ± 0.006	3.0 ± 0.8
				0.031 ± 0.008	4.0 ± 0.4
Lezo	*Estuary*	1	Low	0.11 ± 0.01	0.68 ± 0.04
				0.011 ± 0.004	0.60 ± 0.05
			High	0.049 ± 0.003	0.63 ± 0.03
				0.057 ± 0.003	0.44 ± 0.02
		3	Low	0.026 ± 0.022	0.22 ± 0.06
				0.034 ± 0.003	0.14 ± 0.03
			High	0.030 ± 0.014	0.50 ± 0.11
				0.050 ± 0.020	0.57 ± 0.18

Concentrations of Cd and Pb at Fal Estuary, southern England

Table 3.4 documents Cd and Pb concentrations in water sampled at the Falmouth site. Here, variance was noted in the concentrations detected between the two sampling days, which was not observed in other sites. Cd and Pb concentrations appear to be increased on Day 3, and this increase is significant ($p < 0.05$) for Cd. There is an apparent increase in Pb concentration during high tide on Day 3, but this is only present as a single replicated set and conclusions cannot be drawn.

Table 3.4. Cd and Pb concentrations measured by ASV (documented in Table 3.1) at Falmouth, southern England.

Site Name	Type	Day	State of Tide	Cd concentration (μg/L)	Pb concentration (μg/L)
Fal	*Estuary*	1	Low	<LD	0.17 ± 0.01
				<LD	0.19 ± 0.01
			High	0.017 ± 0.008	0.13 ± 0.01
				<LD	0.091 ± 0.017
		3	Low	0.026 ± 0.022	0.22 ± 0.06
				0.034 ± 0.003	0.14 ± 0.03
			High	0.030 ± 0.014	0.50 ± 0.11
				0.050 ± 0.020	0.57 ± 0.18

Concentrations of Cd and Pb at Atlantic coastal French locations

The concentrations of Cd and Pb found at the three sampled Atlantic coastal French sites are shown in Table 3.5. These sites each exhibited low levels of Cd and Pb, despite the spatial resolution of the sites—the two sites closest to each other, Saumonard and Saint-Nazaire, are approximately 160 km apart, and Port En Bessin is located in the English Channel at the north of France. Pb concentrations showed no significant variation between sites ($p > 0.05$) but were significantly lower than the estuarine sites sampled in England and Spain ($p < 0.05$).

Table 3.5. Cd and Pb concentrations measured by ASV (documented in Table 3.1) at three sampled Atlantic coastal French sites.

Site Name	Type	Day	State of Tide	Cd concentration (μg/L)	Pb concentration (μg/L)
Saumonard	*Coastal*	1	N/A	<LD	0.084 ± 0.018
				0.013 ± 0.010	0.13 ± 0.01
		3	N/A	<LD	0.066 ± 0.024
				<LD	0.10 ± 0.03
Saint-Nazaire	*Coastal*	3	N/A	0.037 ± 0.015	0.068 ± 0.008
				0.028 ± 0.020	0.15 ± 0.02
Port En Bessin	*Coastal*	1	N/A	<LD	0.054 ± 0.014
				0.013 ± 0.012	0.079 ± 0.015
		3	N/A	0.051 ± 0.022	1.1 ± 0.1
				0.034 ± 0.008	0.026 ± 0.01

Concentrations of Ni at selected sites and ICP comparison

Based on the findings of the previous analyses, a number of sites were selected from each region to analyse DMG-complexed Ni concentrations. Samples were treated as

discussed in the Nickel Analysis section of Methods. The results are displayed in Table 3.6. Ni concentrations at the coastal Saint-Nazaire are significantly higher than those at the estuarine sites ($p < 0.05$). However, due to the small number of sites and the extent of variation between replicates, it is challenging to draw conclusions from this data. However, as DMG-complexed Ni should be representative of total Ni in solution, this data may be compared to ICP samples collected simultaneously. Comparison between the two methods, with outliers removed, is displayed in Figure 3.6.

Table 3.6. Ni concentrations by cathodic AdSV (following procedures in Table 3.1) at selected sites from the study regions.

Site Name	Type	Day	State of Tide	Ni concentration (µg/L)
Museo	*Estuary*	1	Low	0.30 ± 0.02
				0.34 ± 0.04
		1	High	0.27 ± 0.25
				1.12 ± 0.18
		3	Low	0.61 ± 0.06
				0.43 ± 0.01
		3	High	1.50 ± 0.22
				0.71 ± 0.07
Fal	*Estuary*	1	Low	0.86 ± 0.21
				0.52 ± 0.05
		1	High	0.67 ± 0.14
				0.30 ± 0.03
Saint-Nazaire	*Coastal*	3	N/A	2.0 ± 0.2
				2.7 ± 0.3

Figure 3.6. Comparison between Ni concentrations by ICP-MS and Ni concentrations by DMG complexation and cathodic AdSV.

3.4 Discussion

3.4.1 CRM Recoveries

Example recoveries of trace metals present in CRMs used for validation of this method are presented in Table 3.2. It would be expected that the ASV method employed for Cd & Pb analysis should represent the labile fraction, while DMG-complexed Ni by cathodic AdSV should represent the total dissolved fraction. While recoveries which were within a reasonable range were obtained for Cd and Ni, Pb was difficult to measure accurately at the low concentrations of CASS-6 and SLEW-3. As will be discussed in Section 3.4.2, the LOD for Pb via the employed method was 0.008 µg/L, within the error range of both CASS-6 and SLEW-3 Pb concentrations. At this low level, background noise contributes to the shape of the peak causing spikes and dips within the peak, and reproducibility is challenged. An example replicate of SLEW-3 is included in Figure 3.7. However, at concentrations of approximately 0.04 µg/L Pb, the Pb peak is well resolved from the background noise.
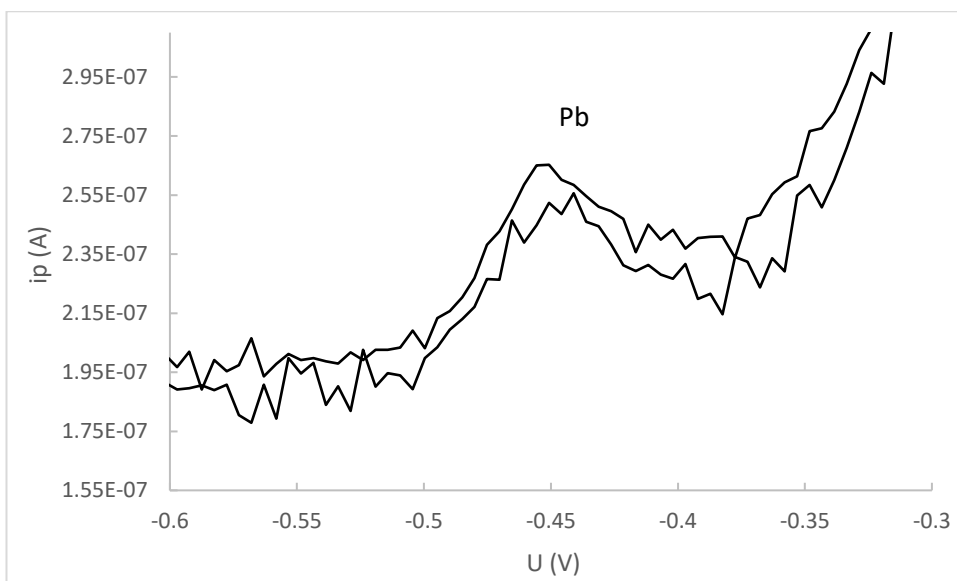
Figure 3.7. Replicates of the SLEW-3 CRM (Pb concentration 0.009 ± 0.004 µg/L) by ASV using operating conditions in Table 3.1 prior to standard addition. The impact of background noise on peak shape can here be observed.

3.4.2 Limits of Detection

LOD was calculated for each sample using Equation 6, as documented in the Appendix. During analysis of each sample, LOD was calculated and was used as a secondary validation method, by comparing sample detection limits to instrumental detection limits for a given standard addition concentration. Instrumental detection limits were derived daily by performing standard additions on an 18.2 MΩ deionised water blank. For Cd and Pb, these limits were 0.006 and 0.008 µg/L respectively for standard addition concentrations of 12 µg/L. For Ni, LOD was typically below 0.02 µg/L for 30 and 40 µg/L standard addition concentrations. In the majority of samples analysed, sample LOD did not deviate greatly from these instrumental values (for the Oiartzun River sites Museo and Lezo, Cd LOD was approximately 0.009 µg/L). In cases where a significant increase in the detection limit was noted, the measurement was repeated after re-coating the electrode with a mercury film if it was suspected to be damaged, or following UV irradiation of the sample if excess DOM in the sample adsorbing to the electrode was suspected.

3.4.2 Sonication of glassy carbon electrode

Initially in this research, the sonication step of the GCE preparation protocol for Cd and Pb analysis was excluded, being deemed ineffective or potentially detrimental to the longevity of the electrode. Zhang & Coury investigated the effect of sonication on GCEs, and found that following sonication in water, no enhancement of signal was noted.[154] Pitting on the surface of the electrode was increased in water when compared to dioxane, and more electrochemically active oxides were noted at the electrode surface. However, surface defects are often desirable for mercury film deposition, as it provides more nucleation sites for mercury cation adsorption than a highly polished electrode.[155] The surface of an electrode is typically not homogenous, with pits, cracks and raised features being present on the surface of an unpolished electrode.[134] In this procedure, the electrode is polished to reduce the surface heterogeneity and then is sonicated to provide more homogenous pitting across the entire electrode working surface.

3.4.3 The use of two methods for trace metal analysis

In this investigation, Ni analysis is conducted by cathodic AdSV following DMG complexation, while Cd and Pb analysis is conducted using ASV methods. All three metals were initially analysed using a HMDE, but in the case of Cd and Pb, it was found that the LOD was not sufficiently low for the analysis of uncontaminated coastal or estuarine waters. For these two metals, the MFE was employed, as the method can achieve detection limits an order of magnitude lower than the HMDE.[138] The larger surface area of the exposed film when compared to the surface area of the 1 mm diameter mercury drop allows for improved efficiency of preconcentration and higher sensitivity.[133] As the Ni concentrations in uncontaminated samples are higher, the HMDE is preferable for Ni analysis due to the reduced setup time, and the ability to clean the electrode easily by purging the drop between samples. Despite the sensitivity of MFE, it is a more vulnerable method due to the possibility of damage of the mercury film and the incomplete stripping of analytes or organic matter adsorption, reducing the number of analyses that can be reliably completed before the film requires replacement.[134]

Analysis of all three metals examined in this study is possible using mercury electrode with mixes of DMG and 8-hydroxyquinoline as described by Colombo & Van Den

Berg.[156] However, this simultaneous analysis raises the detection limits of all analytes, reducing the sensitivity for Cd and Pb quantitation by up to 50% when performing analysis of all three metals of interest. Excess Cu in the solution under this protocol also supresses Pb peaks. As has been seen, the low concentrations of Pb found in the CRMs are challenging to quantitate even in a method optimised for Pb, and the impact of these further suppressions would have dramatically increased detection limits. Due to the unknown status of each sample, and the necessity to optimise detection limits for each metal, Ni analysis was performed separately to preserve sensitivity of Cd and Pb detection.

3.4.4 Outlier and Suspect Data

Some sample replicates in Tables 3.2-3.6 exhibited discrepancies in total metal concentrations. These sample replicates include Port En Bessin Day 3, and Museo Day 1, High Tide, the latter of which exhibited observable differences in all three analysed metals. In the case of these samples, analysis was repeated on both samples using a newly prepared mercury film to eliminate incomplete stripping or insufficient cleaning between samples as a potential source of contamination. The heightened concentrations in these samples persisted between runs, however. As the water in both replicates was taken directly from the same sampling vessel, and acidified similarly in each case, sample preparation and filtration was the main potential source of contamination. The filtration process, performed on-site and validated using field blanks of deionised water filtered similarly, was used to remove sediment and other particulate from water samples prior to acidification. Excessive agitation of the sample vessel during filtration may have resulted in resuspension of adsorbed trace metal from sediment to solution. The samples were filtered by hand, using a syringe to induce a vacuum, and as such error may have been introduced during this manual handling. For future analysis, use of a small portable vacuum system which can keep the sample stable during filtration may be preferable.

Outlier testing was performed on suspect data points using Grubbs' Test on all samples for the site in question. Museo Day 1, High Tide data for Cd, Pb and Ni was deemed to be within an acceptable value for the range and was retained for further analysis. The high Pb level noted in one replicate at Port En Bessin, Day 3, was deemed to be an outlier and excluded from the dataset for further consideration.

3.4.5 Cd and Pb as Environmental Contaminants

Under the WFD, Cd and Pb have been included as priority substances and must be monitored as contaminants of emerging concern.[10] In this study, contamination by these trace metals at the majority of sampled sites appears to be minimal. Of all the samples analysed, only one Cd sample was in excess of 0.1 μg/L. This level of contamination is below the AA-EQS (Annual Average Environmental Quality Standards) values for Cd for other (non-inland) surface waters (0.2 μg/L).[11] The data from this study suggests that there is no major ecological concern with respect to Cd at the sampled locations. The sites which are further inland and closer to towns (Lezo on the Oiartzun River, and Port En Bessin and Saint-Nazaire on the French coast) exhibited higher Cd concentrations than those at transitional waterways or coastal waters (Museo and Saumonard respectively). This may be in part due to input of municipal wastewater effluent into the waterway.

For Pb contamination, while most site concentrations are below the WFD AA-EQS guidelines for Pb non-inland surface waters (1.3 μg/L), the Pb concentration values at Museo are in excess of AA-EQS in all cases, but below the WHO's drinking water guidelines of 5 μg/L Pb.[11,157] The high concentrations noted at Museo at each day at both tidal variations indicates an ongoing pollution issue during the study. This occurred at some point in the watercourse between the Museo sampling site and Lezo, which was comparatively significantly less contaminated. Anthropogenic industrial inputs along the course of the Oiartzun river may be causing a continuous contamination issue with respect to Pb. Some trace metal concentration values at the site exceed 4 μg/L, and further increases in these concentrations could have detrimental impacts on the environmental status of the river and should be monitored closely. However, the low temporal resolution of this study means that it is challenging to determine if this contamination event was restricted to the sampling period or if it is continuous.

Waters in the Oiartzun river have previously been characterised using DGT passive sampling devices by Montero *et al.*[13] Concentrations of Cd and Pb measured following ten-day averaged deployments of DGTs had maximums of 286 and 78 ng/L respectively. The study conducted here found maximum concentrations of Cd and Pb of 60 ng/L and 4300 ng/L, respectively. DGTs typically measure a wider range of metal species (including larger labile organic complexes) than ASV or CSV on filtered

water, which may contribute to the lower Cd results obtained in this study. However, the contamination at Museo is significantly and consistently higher in this study, indicating a potential contamination issue as of this study period (September 2018).

3.4.6 Ni as an Environmental Contaminant

Ni is documented under the WFD as a priority substance which must be monitored, and sources of contamination mediated.[10] While the biological half-life of Ni is not as long as Cd and Pb, which can persist in biotic tissue for years to decades, Ni can result in respiratory damage following acute contamination events. In this study, the Ni concentrations found at the studied sites were all below the AA-EQS values of Ni for non-inland waters (8.6 μg/L).[4] Ni at Saint-Nazaire was significantly higher than the other sites examined ($p < 0.05$). Despite these higher concentrations at Saint-Nazaire, the data from the selected sites suggest that there is no ecological concern for acute Ni contamination during the study period. However, the small number of samples and restricted temporal distribution of this study should be considered.

3.4.7 Application of Stripping Voltammetry to Low-Level Trace Analysis

This chapter has adapted and applied methods for trace analysis of Ni, Cd, and Pb from previous authors. Here, lower levels of metals were considered in many cases, and were applied to a number of estuarine and coastal sites across the Atlantic coast. However, challenges were identified with the generation of results at these low levels. As discussed in Section 3.4.1, low concentrations of Pb in the CRMs used for method validation could not be accurately and reliably quantified. The interference of background noise in voltammograms was prevalent in samples below labile Pb concentrations of 0.04 μg/L. More concentrated solutions, such as those obtained at the Museo site, correlate more closely with values measured by other methods.[151]

A small number of DMG-complexed Ni samples were analysed and while some correlated closely with total metals as analysed by ICP, variance between replicates was noted. Notably, the sample from Saint-Nazaire exhibited concentrations three times higher than ICP when analysed by cathodic AdSV. This may have been the result of operator error, as Cobelo-García *et al.* successfully applied the method to analyse Ni concentrations in coastal waters at the site of an oil spill.[152] However, slight differences in the protocols for sample handling between ICP and voltammetry

samples in the present study may have contributed slightly to differences. While voltammetry samples were filtered and acidified onsite, ICP samples were stored under refrigerated conditions until being frozen, and were subsequently thawed, filtered, and acidified. While this may have resulted in some labile Ni being bound to particulate matter during storage and subsequently filtered from the sample, it is unlikely this would have resulted in the large discrepancies between some samples. The variance between replicates observed in this study is indicative of difficulty encountered when running samples at the low concentrations of uncontaminated waters.

3.5 Conclusion

In this study, the labile Cd, Pb, and Ni concentrations at six coastal and transitional waterways were examined using ASV and cathodic AdSV. In most cases, low concentrations of these trace elements were detected, below the EU WFD's guideline levels for non-inland water sources.[11] The Oiartzun river, despite effective remediation projects in controlling Cd and Ni contamination, exhibited Pb concentrations greater than the WFD's Annual Average Environmental Quality Standard values (1.3 µg/L) across the duration of this study at the Museo site, near to Pasaia. Further study would be required to evaluate the extent of this contamination event over a longer temporal distribution, employing longer-term analysis methods such as sediment trace metal analysis, passive sampling, and tissue sampling of local biota such as mussels or oysters.

The application of ASV and cathodic AdSV, here applied to environmental sites, showed that the method as conducted was not optimised for the detection of low-level Pb contamination, as found in the CRMs for near-shore and estuarine seawater used in this study. In addition, under this study, Ni analysis of each sample did not consistently agree between replicates. While the developments in this chapter further the use of stripping voltammetry for trace metal analysis in environmental water samples, continued optimisation is required to overcome the challenges encountered herein.

Chapter 4

Conclusions and Future Work

4.1 Recommendations for Future Work

This thesis has focused on the investigation of trace metal monitoring and analytical methods, and exploration of a commonly cited limitation of passive sampling devices (impact of biofouling in environmental waters). The definition of Environmental Quality Standards (EQS) for the DGT device in coastal and transitional waterways was highlighted in Chapter 1 as critical for the application of such passive sampling devices in a regulatory context. Such a project would be outside the scope of this research and is currently being undertaken under an international research consortium (MONITOOL Project).[158]

Chapter 1 highlights a necessity to further validate the relationship between DGT-labile metal concentrations and the internalised metal concentrations of bioaccumulator organisms. Of particular interest for the validation of DGT-labile fractions is the use of phytoplanktonic communities as discussed by authors such as Bradac *et al.* and Mangal *et al.*[46,90] At present the relationship between the two sampling methods has only been examined for two metals (Cd and V) in a selected diatom and a wild community, but shows promise that there is a close relationship even when wild communities are examined. Common bioaccumulator macroorganisms such as macrophyta and bivalves also require further validation, but the complexity of their uptake and regulation patterns makes direct comparison challenging. The use of these organisms in ecotoxicity assays with DGT measurement, however, may inform development of accurate DGT-EQS values. DGT presents itself as a useful tool to standardize trace metal contamination measurement across wide geographical regions, removing variation as a result of biomonitor organism selection.

Chapter 2 explores the fouling of DGT device membranes (made of polyethersulphone) by freshwater and marine diatoms, as this could impact on the accuracy of the metal concentrations determined by DGTs for trace metal monitoring. While in this body of work, the PES membrane is explored exclusively, the preferential adhesion of fouling diatoms to different substrates is another factor to be considered when assessing biofouling communities. Future work in this area should incorporate alternative DGT membranes such as polycarbonate (PC) and window surfaces for optical sensors such as PMMA and glass. Such materials were deployed simultaneously with PES under the 14-day deployments discussed in Chapter 2 and

can highlight the different impact of fouling organisms on different substrates and further strengthen the geographical maps developed in this chapter.

Chapter 3 examines the analysis of priority metals in coastal and transitional waters under the Water Framework Directive using stripping voltammetry. Here, detection limits of ng/L were achieved through the adaptation of methods for Cd, Pb and Ni analysis by ASV and cathodic AdSV. However, accurate measurement of low concentrations of Pb, as was found in the Certified Reference Materials used for validation, and the reproducibility of Ni voltammograms were limitations of these adaptations. Further optimization is required to develop the method to reliably quantify Pb at the low levels of pristine environmental waters and to ensure reproducibility for DMG-complexed Ni.

4.2 Conclusions

As trace metals continue to be studied as contaminants of emerging concern, the use of new tools and the optimization of analytical techniques will be critical for the full implementation of regulatory policies such as the Water Framework Directive. Here, emphasis is place on low-cost and easy-to-use methods such as passive sampling devices including DGT devices and analytical techniques such as stripping voltammetry. DGT currently represents a relatively accurate assessment of bioavailable trace metals when compared to certain organisms (Pb in seagrasses, macroalgae and bivalves, and Cd and V in phytoplankton), which approximate the labile metals concentration in the water column. However, further research is required to determine appropriate EQS for DGT-labile metal concentrations under the WFD for the use of the device. Analysis of the concentrations of DGT-labile metals could be performed by the use of stripping voltammetry, allowing for sufficiently low detection limits for analysis of even non-contaminated seawater. Finally, the fouling environments across the Atlantic coast and in the Mediterranean were studied. Findings suggest a limited DGT deployment period of approximately 4-5 days to mitigate the potential impacts of biofouling on device performance. This work stands to help inform future research using passive sampling or stripping voltammetry by providing a framework of validation and mitigation of commonly reported limitations of the methods, enabling their incorporation into routine monitoring programs.

References

1   P. B. Tchounwou, C. G. Yedjou, A. K. Patlolla and D. J. Sutton, in *NIH Public Access*, 2012, pp. 133–164.

2   C. Pergent-Martini and G. Pergent, *Int. J. Environ. Pollut.*, 2000, **13**, 126.

3   D. Sánchez-Quiles, N. Marbà and A. Tovar-Sánchez, *Sci. Total Environ.*, 2017, **576**, 520–527.

4   O. Solaun, J. G. Rodríguez, A. Borja, M. González and J. I. Saiz-Salinas, *Mar. Pollut. Bull.*, 2013, **67**, 26–35.

5   R. R. Philipps, X. Xu, R. B. Bringolf and G. L. Mills, *Environ. Toxicol. Chem.*, 2019, **38**, 61–70.

6   M. Sugita, *Int. Arch. Occup. Environ. Health*, 1978, **41**, 25–40.

7   Basri, M. Sakakibara, K. Sera and I. A. Kurniawan, *Geosciences*, 2017, **7**, 133.

8   K. S. Egorova and V. P. Ananikov, *Organometallics*, 2017, **36**, 4071–4090.

9   R. Chiarelli and M. C. Roccheri, *Open J. Met.*, 2014, **04**, 93–106.

10   European Commission, *Off. J. Eur. Parliam.*, 2000, **L327**, 1–82.

11   European Commission, *Off. J. Eur. Union*, 2013, **L226**, 1–17.

12   N. Simboura, A. Pavlidou, J. Bald, M. Tsapakis, K. Pagou, C. Zeri, A. Androni and P. Panayotidis, *Ecol. Indic.*, 2016, **70**, 89–105.

13   N. Montero, M. J. Belzunce-Segarra, A. Del Campo, J. M. Garmendia, L. Ferrer, J. Larreta, M. González, M. A. Maidana and M. Espino, *J. Mar. Syst.*, 2013, **109–110**, S252–S260.

14   M. A. Schlacher-Hoenlinger and T. A. Schlacher, *Mar. Biol.*, 1998, **131**, 401–410.

15   D. D. Runnells, T. A. Shepherd and E. E. Angino, *Environ. Sci. Technol.*, 1992, **26**, 2316–2323.

16   G. M. McMurtry, J. C. Wiltshire and J. P. Kauahikaua, *Pacific Sci.*, 1995, **49**, 452–470.

17   S. Li and Q. Zhang, *J. Hazard. Mater.*, 2010, **181**, 1051–1058.

18   A. K. Papafilippaki, M. E. Kotti and G. G. Stavroulakis, *Glob. NEST J.*, 2013,

10, 320–325.

19   J. A. Prange and W. C. Dennison, *Mar. Pollut. Bull.*, 2000, **41**, 327–336.

20   P. Buat-Ménard and M. Arnold, *Geophys. Res. Lett.*, 1978, **5**, 245–248.

21   S. Moune, P.-J. Gauthier and P. Delmelle, *J. Volcanol. Geotherm. Res.*, 2010, **193**, 232–244.

22   L. J. Spokes and T. D. Jickells, *Aquat. Geochemistry*, 1996, **1**, 355–374.

23   S. Illuminati, A. Annibaldi, C. Truzzi and G. Scarponi, *Mar. Pollut. Bull.*, 2016, **111**, 476–482.

24   N. J. Valette-Silver, S. B. Bricker and W. Salomons, *Estuaries*, 1993, **16**, 577–588.

25   C. M. Shy, *World Heal. Stat. Q.*, 1990, **43**, 168–176.

26   European Commission, *Off. J. Eur. Communities*, 1998, **L350**, 58–67.

27   A. E. Shiel, D. Weis, D. Cossa and K. J. Orians, *Geochim. Cosmochim. Acta*, 2013, **121**, 155–167.

28   E. D. Goldberg, *Environ. Sci. Policy Sustain. Dev.*, 1986, **28**, 17–44.

29   K. Schiff, D. Diehl and A. Valkirs, *Mar. Pollut. Bull.*, 2004, **48**, 371–377.

30   J. Webb and M. Keough, *Sci. Total Environ.*, 2002, **298**, 207–217.

31   O. Bajt, A. Ramšak, V. Milun, B. Andral, G. Romanelli, A. Scarpato, M. Mitrić, T. Kupusović, Z. Kljajić, M. Angelidis, A. Çullaj and F. Galgani, *Mar. Pollut. Bull.*, 2019, **141**, 283–298.

32   D. A. Steffy, A. C. Nichols, L. J. Morgan and R. Gibbs, *Water, Air, Soil Pollut.*, 2013, **224**, 1756.

33   D. Roberts, L. Shiels, J. Tickle, R. de Nys and N. Paul, *Water*, 2018, **10**, 626.

34   G. Roca, J. Romero, S. Farina, B. Martínez-Crego and T. Alcoverro, *Mar. Pollut. Bull.*, 2017, **123**, 83–91.

35   Z. Dragun, B. Raspor and V. Roje, *Chem. Speciat. Bioavailab.*, 2008, **20**, 33–46.

36   E. Garofalo, S. Ceradini and M. Winter, *Ann. Chim.*, 2004, **94**, 515–520.

37   I. J. Allan, J. Knutsson, N. Guigues, G. A. Mills, A.-M. Fouillac and R.

Greenwood, *J. Environ. Monit.*, 2008, **10**, 821.

38 M. Senila, E. A. Levei, L. R. Senila and M. Roman, *J. Chem.*, 2015, **2015**, 1–8.

39 H. E. Allen and D. J. Hansen, *Water Environ. Res.*, 1996, **68**, 42–54.

40 A. Turner, S. S. Pedroso and M. T. Brown, *Mar. Chem.*, 2008, **110**, 176–184.

41 A.-M. Cindrić, N. Cukrov, G. Durrieu, C. Garnier, I. Pižeta and D. Omanović, *Croat. Chem. Acta*, 2017, **90**, 177–185.

42 A. Turner, M. Nimmo and K. A. Thuresson, *Mar. Chem.*, 1998, **63**, 105–118.

43 C. M. Zhao, P. G. C. Campbell and K. J. Wilkinson, *Environ. Chem.*, 2016, **13**, 425–433.

44 P. Malea, *Bot. Mar.*, 1993, **36**, 423–432.

45 E. D. Amato, C. P. M. Marasinghe Wadige, A. M. Taylor, W. A. Maher, S. L. Simpson and D. F. Jolley, *Environ. Pollut.*, 2018, **243**, 862–871.

46 P. Bradac, E. Navarro, N. Odzak, R. Behra and L. Sigg, *Environ. Toxicol. Chem.*, 2009, **28**, 2108–2116.

47 J. Søndergaard, G. Asmund and M. M. Larsen, *MethodsX*, 2015, **2**, 323–330.

48 T. Sumida, T. Nakazato, H. Tao, M. Oshima and S. Motomizu, *Anal. Sci.*, 2006, **22**, 1163–1168.

49 P. L. Brezonik, P. A. Brauner and W. Stumm, *Water Res.*, 1976, **10**, 605–612.

50 R. J. K. Dunn, P. R. Teasdale, J. Warnken and R. R. Schleich, *Environ. Sci. Technol.*, 2003, **37**, 2794–2800.

51 C. Vale, *Sci. Total Environ.*, 1990, **97–98**, 137–154.

52 G. Bonanno and M. Orlando-Bonaca, *Sci. Total Environ.*, 2018, **618**, 1152–1159.

53 C. Lafabrie, G. Pergent, R. Kantin, C. Pergent-Martini and J.-L. Gonzalez, *Chemosphere*, 2007, **68**, 2033–2039.

54 E. D. Amato, S. L. Simpson, M. J. Belzunce-Segarra, C. V. Jarolimek and D. F. Jolley, *Environ. Sci. Technol.*, 2015, **49**, 14204–14212.

55 M. Vannuci-Silva, J. M. de Souza, F. F. de Oliveira, M. A. G. de Araújo, E. Francioni, C. E. Eismann, C. H. Kiang, J. S. Govone, M. J. Belzunce-Segarra

and A. A. Menegário, *Water, Air, Soil Pollut.*, 2017, **228**, 222.

56   S. L. Simpson, H. Yverneau, A. Cremazy, C. V. Jarolimek, H. L. Price and D. F. Jolley, *Environ. Sci. Technol.*, 2012, **46**, 9038–9046.

57   Y. Dai, M. Nasir, Y. Zhang, H. Wu, H. Guo and J. Lv, *Sci. Rep.*, 2017, **7**, 14206.

58   T. Zalewska and B. Danowska, *Mar. Pollut. Bull.*, 2017, **118**, 281–288.

59   P. S. Rainbow, *Mar. Pollut. Bull.*, 1995, **31**, 183–192.

60   R. Wilkes, M. Bennion, N. McQuaid, C. Beer, G. McCullough-Annett, K. Colhoun, R. Inger and L. Morrison, *Ecol. Indic.*, 2017, **82**, 117–130.

61   R. Tolotti, S. Consani, C. Carbone, G. Vagge, M. Capello and L. Cutroneo, *J. Environ. Sci.*, 2019, **75**, 233–246.

62   M. Schintu, B. Marras, L. Durante, P. Meloni and A. Contu, *Environ. Monit. Assess.*, 2010, **167**, 653–661.

63   J. Søndergaard, L. Bach and K. Gustavson, *Mar. Pollut. Bull.*, 2014, **78**, 102–109.

64   W. Davison and H. Zhang, *Environ. Chem.*, 2012, **9**, 1.

65   M. E. Conti, M. B. Tudino, M. G. Finoia, C. Simone and J. Stripeikis, *Ecol. Indic.*, 2019, **104**, 296–305.

66   J. A. Webb and M. J. Keough, *Mar. Pollut. Bull.*, 2002, **44**, 222–229.

67   N. Bax, A. Williamson, M. Aguero, E. Gonzalez and W. Geeves, *Mar. Policy*, 2003, **27**, 313–323.

68   L. A. Zimmer, G. Asmund, P. Johansen, J. Mortensen and B. W. Hansen, *Polar Biol.*, 2011, **34**, 431–439.

69   C. de Mestre, W. Maher, D. Roberts, A. Broad, F. Krikowa and A. R. Davis, *Mar. Pollut. Bull.*, 2012, **64**, 80–89.

70   M. Randone, G. Di Carlo and M. Costantini, *Reviving the Economy of the Mediterranean Sea: Actions for a Sustainable Future*, 2017.

71   R. J. Lawton, R. de Nys, S. Skinner and N. A. Paul, *PLoS One*, 2014, **9**, e90223.

72   K. Kilminster, *Mar. Pollut. Bull.*, 2013, **73**, 381–388.

73   C.-F. Boudouresque, G. Bernard, P. Bonhomme, E. Charbonnel, G. Diviacco, A.

Meinesz, G. Pergent, C. Pergent-Martini, S. Ruitton and L. Tunesi, *Protection and conservation of Posidonia oceanica meadows*, 2012.

74   V. Pasqualini, C. Pergent-Martini, P. Clabaut and G. Pergent, *Estuar. Coast. Shelf Sci.*, 1998, **47**, 359–367.

75   J. Richir, N. Luy, G. Lepoint, E. Rozet, A. Alvera Azcarate and S. Gobert, *Aquat. Toxicol.*, 2013, **140–141**, 157–173.

76   M. Bonacorsi, C. Pergent-Martini, N. Breand and G. Pergent, *Mediterr. Mar. Sci.*, 2013, **14**, 193.

77   G. Jordà, N. Marbà and C. M. Duarte, *Nat. Clim. Chang.*, 2012, **2**, 821–824.

78   H. Zhang and W. Davison, *Anal. Chem.*, 1995, **67**, 3391–3400.

79   W. Davison and H. Zhang, *Nature*, 1994, **367**, 546–548.

80   DGT Research Ltd., Diffusion Coefficients in the standard DGT gel (agarose crosslinked polyacrylamide, APA), https://www.dgtresearch.com/diffusion-coefficients/, (accessed 18 December 2019).

81   H. Zhang and W. Davison, *Environ. Chem.*, 2015, **12**, 85.

82   S. Ding, D. Xu, Q. Sun, H. Yin and C. Zhang, *Environ. Sci. Technol.*, 2010, **44**, 8169–8174.

83   C. Zhang, S. Ding, D. Xu, Y. Tang and M. H. Wong, *Environ. Monit. Assess.*, 2014, **186**, 7367–7378.

84   K. E. Brodersen, K. Koren, M. Moßhammer, P. J. Ralph, M. Kühl and J. Santner, *Environ. Sci. Technol.*, 2017, **51**, 14155–14163.

85   P. Diviš, J. Machát, R. Szkandera and H. Dočekalová, *Int. J. Environ. Res.*, 2012, **6**, 87–94.

86   S. Wang, Z. Wu and J. Luo, *Environ. Sci. Technol.*, 2018, **52**, 1096–1108.

87   M. Schintu, L. Durante, A. Maccioni, P. Meloni, S. Degetto and A. Contu, *Mar. Pollut. Bull.*, 2008, **57**, 832–837.

88   R. C. Playle, D. G. Dixon and K. Burnison, *Can. J. Fish. Aquat. Sci.*, 1993, **50**, 2678–2687.

89   C. D. Luider, J. Crusius, R. C. Playle and P. J. Curtis, *Environ. Sci. Technol.*, 2004, **38**, 2865–2872.

90   V. Mangal, Y. Zhu, Y. X. Shi and C. Guéguen, *Chemosphere*, 2016, **163**, 90–98.

91   W. Baeyens, Y. Gao, W. Davison, J. Galceran, M. Leermakers, J. Puy, P. J. Superville and L. Beguery, *Sci. Rep.*, 2018, **8**, 1–11.

92   L. F. Melo and T. R. Bott, *Exp. Therm. Fluid Sci.*, 1997, **14**, 375–381.

93   C. Compère, M. N. Bellon-Fontaine, P. Bertrand, D. Costa, P. Marcus, C. Poleunis, C. M. Pradier, B. Rondot and M. G. Walls, *Biofouling*, 2001, **17**, 129–145.

94   R. M. Donlan, *Emerg Infect Dis.*, 2002, **8**, 881–890.

95   G. S. Lorite, C. M. Rodrigues, A. A. de Souza, C. Kranz, B. Mizaikoff and M. A. Cotta, *J. Colloid Interface Sci.*, 2011, **359**, 289–295.

96   S. Kjelleberg, B. A. Humphrey and K. C. Marshall, *Appl. Environ. Microbiol.*, 1982, **43**, 1166–72.

97   T. Nguyen, F. A. Roddick and L. Fan, *Membranes (Basel).*, 2012, **2**, 804–840.

98   A. J. Martín-Rodríguez, J. M. F. Babarro, F. Lahoz, M. Sansón, V. S. Martín, M. Norte and J. J. Fernández, *PLoS One*, 2015, **10**, e0123652.

99   M. E. Callow, J. A. Callow, J. D. Pickett-Heaps and R. Wetherbee, *J. Phycol*, 1997, **33**, 938–947.

100   D. Roberts, D. Rittschof, E. Holm and A. R. Schmidt, *J. Exp. Mar. Bio. Ecol.*, 1991, **150**, 203–221.

101   N. J. O'Connor and D. L. Richardson, *J. Exp. Mar. Bio. Ecol.*, 1996, **206**, 69–81.

102   D. Sell, in *Marine fouling. Proceedings of the Royal Society of Edinburgh. Section B. Biological Sciences*, 1992, pp. 169–184.

103   F. E. Round, R. M. Crawford and D. G. Mann, *The Diatoms: Biology & Morphology of the Genera*, 1st edn., 1990.

104   K. Leblanc, J. Arístegui, L. Armand, P. Assmy, B. Beker, A. Bode, E. Breton, V. Cornet, J. Gibson, M. P. Gosselin, E. Kopczynska, H. Marshall, J. Peloquin, S. Piontkovski, A. J. Poulton, B. Quéguiner, R. Schiebel, R. Shipe, J. Stefels, M. A. Van Leeuwe, M. Varela, C. Widdicombe and M. Yallop, *Earth Syst. Sci. Data*, 2012, **4**, 149–165.

105   A. Sournia, M. J. Chrdtiennot-dinet and M. Ricard, *J. Plankton Res.*, 1991, **13**, 1093–1099.

106   M. E. Callow and J. A. Callow, *Biologist*, 2002, **49**, 10–14.

107   P. J. Molino and R. Wetherbee, *Biofouling*, 2008, 24, 365–379.

108   K. D. Hoagland, J. R. Rosowski, M. R. Gretz and S. C. Roemer, *J. Phycol.*, 1993, 29, 537–566.

109   S. Malviya, E. Scalco, S. Audic, F. Vincent, A. Veluchamy, J. Poulain, P. Wincker, D. Iudicone, C. de Vargas, L. Bittner, A. Zingone and C. Bowler, *Proc. Natl. Acad. Sci.*, 2016, **113**, E1516–E1525.

110   B. Censarek and G. Rainer, *Mar. Micropaleontol.*, 2002, **45**, 309–356.

111   A. Kerr, M. J. Cowling, C. M. Beveridge, M. J. Smith, A. C. S. Parr, R. M. Head, J. Davenport and T. Hodgkiess, *Environ. Int.*, 1998, **24**, 331–343.

112   M. Lehaitre, L. Delauney and C. Compère, in *Real-time coastal observing systems for marine ecosystem dynamics and harmful algal blooms : theory, instrumentation and modelling*, UNESCO, 2008, pp. 463–493.

113   A. Whelan and F. Regan, *J. Environ. Monit.*, 2006, **8**, 880.

114   N. Voulvoulis, M. D. Scrimshaw and J. N. Lester, *Appl. Organomet. Chem.*, 2002, **13**, 135–143.

115   L. Delauney, C. Compare and M. Lehaitre, *Ocean Sci.*, 2010, **6**, 503–511.

116   J. A. Callow and M. E. Callow, *Nat. Commun.*, 2011, 2, 210–244.

117   E. Uher, C. Compère, M. Combe, F. Mazeas and C. Gourlay-Francé, *Environ. Sci. Pollut. Res.*, 2017, **24**, 13797–13807.

118   M. W. Mittelman and G. G. Geesey, *Appl. Environ. Microbiol.*, 1985, **49**, 846–851.

119   F. G. Ferris, S. Schultze, T. C. Witten, W. S. Fyfe and T. J. Beveridge, *Appl. Environ. Microbiol.*, 1989, **55**, 1249–57.

120   E. D. Van Hullebusch, M. H. Zandvoort and P. N. L. Lens, *Environ. Sci. Bio/Technology*, 2003, **2**, 9–33.

121   C. Pichette, H. Zhang, W. Davison and S. Sauvé, *Talanta*, 2007, **72**, 716–722.

122   E. Uher, H. Zhang, S. Santos, M. H. Tusseau-Vuillemin and C. Gourlay-Francé,

Anal. Chem., 2012, **84**, 3111–3118.

123 N. S. Webster and A. P. Negri, *Environ. Microbiol.*, 2006, **8**, 1177–1190.

124 M. G. Potapova, A. D. Minerovic, J. Veselá and C. R. Smith, Diatom New Taxon File at the Academy of Natural Sciences (DNTF-ANS), Philadelphia, http://dh.ansp.org/dntf, (accessed 18 December 2019).

125 M. D. Guiry and G. M. Guiry, AlgaeBase, https://www.algaebase.org, (accessed 18 December 2019).

126 J. P. Lord, *Mar. Ecol.*, 2017, **38**, 1–10.

127 N. M. Farhat, J. S. Vrouwenvelder, M. C. M. Van Loosdrecht, S. S. Bucs and M. Staal, *Water Res.*, 2016, **103**, 149–159.

128 L. Oliveira and N. J. Antia, *Br. Phycol. J.*, 1984, **19**, 125–134.

129 B. S. Twining, S. B. Baines, S. Vogt and D. M. Nelson, *Global Biogeochem. Cycles*, 2012, **26**, 1–9.

130 J. Wang, *Environ. Sci. Technol.*, 1982, **16**, 104A-109A.

131 J. L. Vílchez, L. Araujo, A. Prieto and A. Navalón, *J. Pharm. Biomed. Anal.*, 2001, **26**, 23–29.

132 W. F. Smyth, in *Electrochemistry, Sensors and Analysis: Proceedings of the International Conference 'Electroanalysis na hÉireann'*, eds. M. R. Smyth and J. G. Vos, Dublin, 1986, pp. 29–36.

133 A. C. Fisher, *Electrode Dynamics*, 1st edn., 1996.

134 R. G. Compton and C. E. Banks, *Understanding Voltammetry*, 3rd edn., 2018.

135 T. M. Florence, *J. Electroanal. Chem.*, 1972, **35**, 237–245.

136 G. March, T. D. Nguyen and B. Piro, *Biosensors*, 2015, **5**, 241–275.

137 C. M. G. Van Den Berg, *Sci. Total Environ.*, 1986, **49**, 89–99.

138 P. Valenta, L. Mart and H. W. Nürnberg, in *Electrochemistry, Sensors and Analysis: Proceedings of the International Conference 'Electroanalysis na hÉireann'*, eds. M. R. Smyth and J. G. Vos, Dublin, 1986, pp. 13–27.

139 A. Bobrowski, B. Baś, J. Dominik, E. Niewiara, E. Szalińska, D. Vignati and J. Zarębski, *Talanta*, 2004, **63**, 1003–1012.

140   J. Wang, *Analytical Electrochemistry*, Wiley-VCH, Danvers, Second Ed., 2000.

141   M. Ariel and U. Eisner, *J. Electroanal. Chem.*, 1963, **5**, 362–374.

142   J. R. Donat and K. W. Bruland, *Anal. Chem.*, 1988, **60**, 240–244.

143   J. Wang, *Electroanalysis*, 2005, **17**, 1341–1346.

144   D. Zhao, X. Guo, T. Wang, N. Alvarez, V. N. Shanov and W. R. Heineman, *Electroanalysis*, 2014, **26**, 488–496.

145   G. H. Hwang, W. K. Han, J. S. Park and S. G. Kang, *Talanta*, 2008, **76**, 301–308.

146   S. Lee, S. K. Park, E. Choi and Y. Piao, *J. Electroanal. Chem.*, 2016, **766**, 120–127.

147   C. Caplat, H. Texier, D. Barillier and C. Lelievre, *Mar. Pollut. Bull.*, 2005, **50**, 504–511.

148   I. Ascione Kenov, F. Muttin, R. Campbell, R. Fernandes, F. Campuzano, F. Machado, G. Franz and R. Neves, *Estuar. Coast. Shelf Sci.*, 2015, **167**, 32–44.

149   D. Pirrie and R. K. Shail, *Geol. Today*, 2018, **34**, 215–223.

150   S. N. Pedersen and A. K. Lundebye, *Mar. Environ. Res.*, 1996, **42**, 241–246.

151   L. M. De Carvalho, P. C. Do Nascimento, A. Koschinsky, M. Bau, R. F. Stefanello, C. Spengler, D. Bohrer and C. Jost, *Electroanalysis*, 2007, **19**, 1719–1726.

152   A. Cobelo-García, J. Santos-Echeandía, R. Prego and O. Nieto, *Electroanalysis*, 2005, **17**, 906–911.

153   H. B. Xue, S. Jansen, A. Prasch and L. Sigg, *Environ. Sci. Technol.*, 2001, **35**, 539–546.

154   H. Zhang and L. A. Coury, *Anal. Chem.*, 1993, **65**, 1552–1558.

155   W. Frenzel, *Anal. Chim. Acta*, 1993, **273**, 123–137.

156   C. Colombo and C. M. G. van den Berg, *Anal. Chim. Acta*, 1997, **337**, 29–40.

157   World Health Organization, *Guidelines for Drinking-water Quality, Fourth Edition*, 2011.

158   Instituto Tecnológico de Canarias, MONITOOL: New tools for water quality

monitoring, monitoolproject.eu, (accessed 12 December 2019).

Appendix

Generation of confidence intervals from voltammograms (Chapter 3)

Confidence intervals were determined as follows: the averaged addition volume, $\bar{v}_a$ (mL), was subtracted from each added volume, v_a (mL). The sum of these squared results (S) was determined as represented in Equation 2.

$$S = \sum (v_a - \bar{v}_a)^2 \tag{2}$$

The confidence proportion independent of volume and concentration (P_i) was then determined. In Equation 3, $\bar{h}$ represents the average of all average peak heights, m represents the slope and S is determined as in Equation 2.

$$P_i = \sqrt{\frac{\bar{h}^2}{((m^2)(S)) + 0.2}} \tag{3}$$

Equation 4 incorporates concentration of the stock solution, initial volume of solution, slope, and the standard deviation of graphed results (σ) and P_i to determine the concentration dependent confidence interval, P_d.

$$P_d = \frac{\left(\frac{\sigma}{m}\right)(P_i)(C_a)}{v_i} \tag{4}$$

Finally, multiplication of the P_d value by the t_{crit}-value (0.05), allows for generation of a confidence interval, I_c, as in Equation 5.

$$I_c = (t_{crit})(P_d) \tag{5}$$

To calculate the limit of detection (LOD) for each sample, Equation 6 was followed. Three times the standard deviation (SD) of the standard addition series was calculated. Multiplication by C_a and division by the x-variable of the series and the initial addition volume provides the resulting limit of detection in μg/L.

$$LOD = 3\left(\frac{(\sigma)(C_a)}{(x)(v_i)}\right) \qquad (6)$$